Saccharomyces cerevisiae share extracellular vesicles for protection from heat stress

Joshua Oliver

A Thesis

In The Department

of

Biology

Presented in Partial Fulfillment of the Requirements

For the Degree of

Master of Science (Biology) at

Concordia University

Montréal, Quebec, Canada

March 2021

CONCORDIA UNIVERSITY

SCHOOL OF GRADUATE STUDIES

This is to certify that the thesis prepared

By: Joshua Oliver

Entitled: *Saccharomyces cerevisiae* share extracellular vesicles for protection from heat stress

and submitted in partial fulfillment of the requirements for the degree of

Master of Science (Biology)

complies with the regulations of the University and meets the accepted standards with respect to originality and quality.

Signed by the final Examining Committee:

_____ Chair
Dr. William Zerges

_____ External Examiner
Dr. David Kwan

_____ Examiner
Dr. Aashiq Kachroo

_____ Examiner
Dr. William Zerges

_____ Thesis Supervisor
Dr. Christopher Brett

Approved by _____
Dr. Robert Weladji, Graduate Program Director

_____ 2021 _____
Dr. Pascale Sicotte, Dean of Faculty

Abstract

Saccharomyces cerevisiae share extracellular vesicles for protection from heat stress

Joshua Oliver

Proteostasis is partly dependent on quality control mechanisms to detect unfolded proteins and either refold or degrade them. These pathways clear toxic unfolded protein aggregates that appear during aging or under stress for cell survival. However, recent studies suggest that survival of cell populations also rely on extracellular vesicles (EVs) shared under proteotoxic stress. EVs are nanosized lipid membrane-bound carriers of complex biomolecules thought to mediate intercellular communication underlying diverse physiology in humans and across phyla. However, their contributions to proteostasis remain unclear.

Given that the molecular machinery underlying EV biogenesis is conserved in all eukaryotes, I reasoned that *Saccharomyces cerevisiae* (baker's yeast) may serve as a simple model to better understand how EVs may circumvent proteotoxicity in molecular detail. I first optimized methods for isolating and characterizing EVs from yeast by tracking GFP-tagged Bro1, the yeast homolog of ALIX, an established EV biomarker in humans. Using fluorescence microscopy, I show that yeast cells readily share EVs during mild heat stress, and characterize morphology, size and protein content using, scanning probe microscopy, dynamic light scattering and mass spectrometry. Adding these isolated EVs to naïve (unstressed) cells protects them from lethal heat stress. This effect is lost when EVs were collected during osmotic stress or from cells lacking *HSC82* or *SSA2*, genes encoding protein chaperones that are abundant in EVs. I conclude that yeast share EVs containing protein chaperones during heat stress to protect against proteotoxicity for survival, and speculate that EVs may help coordinate proteostasis between cells in all organisms.

Acknowledgements

First and foremost, I would like to thank my supervisor Dr. Christopher Brett for giving me the opportunity of being both a student and a team member of his lab. Through his guidance, strong work ethic and expertise, my passion in research has grown and my future has become all the more clearer and for that I am grateful. Furthermore, I thank my committee members Dr. Aashiq Kachroo and Dr. William Zerges for their unyielding support, research input and time commitment during this project.

I thank Dr. Chris Law, the operations manager and microscope specialist of the Centre for Microscopy and Cellular Imaging at Concordia University. For your swiftness and guidance during technological mishaps and for always providing the reasons why these issues arise and probable solutions. An educational and motivating experience.

To Dr. Heng Jiang, the applications specialist of the Centre for Biological Applications of Mass Spectrometry, I thank you for your meticulous explanations and leadership. It has been an honor collaborating with you.

I would like to thank both past and present members of the Brett Lab for their assistance, moral support and insight. Tom Kazmirchuk, it is with great gratitude I say the following: you are going places and I am looking forward to those days my friend.

Finally, I dedicate this work to my parents for their wisdom, love and laughter.

Contribution of Authors

Figure 1: Claire Staton contributed to the initial designing of the cartoon in A.

Figure 3: Tom Kazmirchuk contributed to the image acquisition as shown in B.

Figure 3: Melissa Magi contributed to the analysis as shown in B.

Figure 6: Claire Staton contributed the dose-response curve as shown in C.

Table of Contents

List of Figures

List of Tables

List of Supplemental Figures

List of Supplemental Tables

List of Abbreviations

AFM	atomic force microscopy
ALIX	apoptosis-linked gene 2–interacting protein X
ATPase	adenosine triphosphatase
BSA	bovine serum albumin
CAP	capsule-associated gene
Cdc42	cell division control protein 42
CSF	cerebrospinal fluid
DC	dendritic cell
DIC	differential interference contrast
DNA	deoxyribonucleic acid
ECM	extracellular matrix
EIF	eukaryotic translation initiation factor
ESCRT	endosomal sorting complexes required for transport
EV	extracellular vesicle
FM4-64	*N*-(3-Triethylammoniumpropyl)-4-(6-(4-(Diethylamino) Phenyl) Hexatrienyl) Pyridinium Dibromide (lipophilic dye for fluorescence microscopy)
GFP	green fluorescent protein
GlcCer	glycosphingolipid glucosylceramide
GXM	glucuronoxylomannan
HILO	highly inclined laminated optical sheet
HSP	heat shock protein
IFN	interferon
IL	interleukin
ILV	intralumenal vesicle
MB	methylene blue
MVB	multivesicular body
NO	nitric oxide
OMV	outer membrane vesicles
PBS	phosphate buffered saline

PC	phosphatidylcholine
PEG	polyethylene glycol
QELS	quasi-elastic light scattering
SC	synthetic complete
SEM	standard error of the mean
TIRF	total internal reflection fluorescence
TLR	toll-like receptor
TNF-α	tumor necrosis factor-alpha
UBD	ubiquitin binding domain
VPS	vacuole protein sorting
YPD	yeast peptone dextrose

Chapter 1: Introduction

1.1 Brief overview of extracellular vesicle physiology

Intercellular communication is a fundamental biological process required for homeostasis of prokaryotic and eukaryotic organisms (Brown et al., 2015; Coelho et al., 2019). In the past few decades, extracellular vesicles (EVs) have emerged as important contributors; however, their physiology remains enigmatic. EV is an umbrella term that defines diverse populations of released lipid-bound vesicles, which differ on the basis of their origin and size. EVs are categorized as ectosomes, exosomes, or apoptotic bodies (Freitas et al., 2019). In brief, ectosomes (or microvesicles) are products of outward budding of the plasma membrane that are released into the extracellular milieu, with diameters ranging between 100 to 1,000 nm (Wu et al., 2017). Exosomes range between 30 to 200 nm in diameter and are derived from endosomal membranes by coordinated activities of ESCRTS, endosomal sorting complexes required for transport (Freitas et al., 2019; Wu et al., 2017). Finally, apoptotic bodies are generated during the disassembly of apoptotic cells and are 500 to 1,000 nm in diameter (Maas et al., 2018). Regardless of type, the principle function of EVs is to sequester and export macromolecules including lipids, proteins, nucleic acids, and carbohydrates into the extracellular space (Oliveira et al., 2010; Kutralam-Munisamy et al., 2015; Toledo Martins et al., 2018) (**Figure 1**).

EVs were originally described as ‘pro-coagulant platelet derived particles’ by Chargaff and West in 1946 when investigating thromboplastic activators within mammalian tissue (Chargaff et al., 1946). In 1967, Peter Wolf observed similar structures following centrifugation of intact platelets which he termed ‘platelet dust’ (Wolf, 1967). In the same decade, bacterial EVs were first described whereby *Escherichia coli*, was reported to ‘pinch off’ EVs from the outer membrane sequestering periplasmic elements; these EVs were termed outer-membrane vesicles (OMVs) (Brown et al., 2015). Further analysis of OMVs showed these vesicles encapsulate diverse cargo such as; virulence factors, DNA, RNA and immunogenic factors involved in biofilm formation, viral propagation, antibiotic resistance and colonization of host tissues (Brown et al., 2015). Similar studies on Gram-positive bacteria were avoided because researchers initially believed their cell walls may physically impede EV release. However, EVs derived from fungal species that possess cell walls were reported in the early 1970s. Images of

the pathogenic fungi *Cryptococcus neoformans* by freeze-etching electron microscopy captured intracellular compartments filled with intralumenal vesicles (ILVs) called, multivesicular bodies (MVBs), appearing to fuse with the plasma membrane to presumably release their contents as EVs (Takeo et al., 1974). Transmission electron micrographs of *Candida albicans* taken later, also suggested EV production via direct budding from the plasma membrane (Anderson et al., 1990). These and other early discoveries demonstrate that EV biogenesis and release seems to be evolutionary conserved among all studied prokaryotic and eukaryotic organisms.

Once released into the extracellular space (interstitial fluid, blood, urine, or the environment), EVs are thought to be recognized by specific cell communities, where their cargo is internalized and elicits diverse responses, depending on composition and target tissue. For example, mammalian EVs are conductors of angiogenesis, glia-neuron communication, tissue development, and metastasis (Wu et al., 2017). Additionally, EVs mediate inter-species or organismal communication. For example, EVs harvested from pathogenic fungi such as *C. neoformans, C. albicans* or *Paracoccidioides brasiliensis* were shown to drive changes in mammalian cell gene expression or prevent host immune cell activation (Nimrichter et al., 2016; Freitas et al., 2019). Thus, in all, fungi seem to be great models to study general EV biology in context to underlying molecular mechanisms, eukaryotic cell physiology, and infectious disease (**Figure 1**).

1.2 EV biogenesis

1.2.1 The ESCRT – dependent biogenic pathway

ESCRTs represent a sequentially acting series of evolutionary conserved multi-protein complexes that drive exosome (a subclass of EVs) biogenesis and supposedly select membrane and lumenal cargo protein composition (Wubbolts et al., 2003; Mears et al., 2004; Gatti et al., 2005; Albuquerque et al., 2008; Rodrigues et al., 2008; Panepinto et al., 2009; Choi et al., 2014; Wang et al., 2019). Endosomes within eukaryotic cells undergo MVB maturation in which four ESCRT complexes (ESCRT-0, I, II, III), accessory proteins (Bro1, Doa4) and ATPase complex

(Vps4) are sequentially recruited to the cytoplasmic face of the endosomal membrane where they drive cargo protein selection and ILV formation (Hessvik et al., 2018). In *Saccharomyces cerevisiae*, ESCRT-0 initiates the exosome biogenesis pathway and is composed of Hse1 and Vps27 (Vacuole Protein Sorting) (Hurley et al., 2010). When recruited to endosomal membranes, the ubiquitin binding domains (UBD) of both subunits recognize and bind ubiquitylated cargo proteins. ESCRT-0 then recruits ESCRT-I complex, consisting of Vps23, Vps28, Vps37 and Mvb12 by interacting with Vps23 (Wollert et al., 2009; Wollert et al., 2010; Hurley et al., 2010). Vps23 and Mvb12 both possess UBDs and Vps28 associates with ESCRT-II, comprised of Vps22, Vps25 and Vps36 via interaction with subunit Vps36 (Katzmann et al., 2001; Kostelansky et al., 2007; Hurley et al., 2010). Vps36 then engages ubiquitylated cargoes while Vps25 recruits ESCRT-III through its interaction with Vps20 (Alam et al., 2004; Hurley et al., 2010).

The final stages of exosome biogenesis involve cargo sequestration and ILV formation; driven by ESCRT-III comprised of Snf7, Vps20, Vps24, and Vps2. Snf7 drives cargo sequestration and interacts with the accessory protein Bro1 to stabilize ESCRT-III ensuring sufficient cargo loading prior to membrane scission (Wemmer et al., 2011). Bro1 also recruits the deubiquitylase Doa4 that removes ubiquitin from cargo (Johnson et al., 2017; Buysse et al., 2020). Bro1 is of particular interest because it is homologous to ALIX (Apoptosis-Linked gene 2–Interacting protein X), an established mammalian exosome biomarker due to its lumenal enrichment specifically within these vesicle subtypes (Mears et al., 2004; Subra et al., 2007; Baietti et al., 2012; Colombo et al., 2013; Yang et al., 2017). Finally, after cargo loading into membrane invaginations encircled by ESCRT-III the Vps4 AAA+ ATPase complex is recruited via Vps2, driving final membrane scission and catalyzing ESCRT disassembly for additional rounds of ILV formation (Babst et al., 2002; Teis et al., 2008). Perimeter membranes of mature MVBs filled with hundreds of ILVs then fuse with the plasma membrane releasing the ILVs as exosomes into the extracellular space.

Although the basis of EV biogenesis remains enigmatic, numerous reports suggested that EVs resembling exosomes can be made without ESCRTs. In *S. cerevisiae*, EVs continue to be secreted in the absence of ESCRT components: deleting *HSE1* (ESCRT-0), *VPS23* (ESCRT-I),

VPS36 (ESCRT-II), *VPS2* (ESCRT-III) or *BRO1* did not inhibit exosome biogenesis, nor did it reduce effects of EVs on recipient cell survival following antifungal treatment (Zhao et al., 2019). Of these, only some mutations seemed to reduce total EV secretion (*VPS2*Δ, *VPS23*Δ), and in all cases the majority of EVs secreted from ESCRT mutants had diameters between 30 - 150 nm, the size of exosomes, although proportionally more large EVs (150 - 500 nm) were observed compared to wild-type cells (Zhao et al., 2019). However, proteomic analysis of isolated EVs revealed that cargo protein content in samples from most ESCRT mutants was different than from wild-type cells. Similar observations were made when *SNF7*, which encodes key component of ESCRT-III, was deleted (Oliveira et al., 2010). Together, these studies suggest that exosomes likely represent at least two EV populations, derived from ESCRT –dependent or –independent processes, that contain different cargo proteins. Thus, EV biosynthesis is not entirely understood in molecular detail warranting further study.

1.3 Fungal EV physiology

Nearly all studies on yeast EV biology address possible roles in virulence when released by pathogenic fungi. This reasoning was originally based on the realization that mammalian EVs seem critical for priming and coordinating cellular activities underlying innate and adaptive immune responses. For example, antigen-specific T cells release EVs containing genomic and mitochondrial DNA that are delivered to dendritic cells (DCs) causing changes in expression of > 1,600 genes including those required for activation of antimicrobial activity (e.g. the interferon (IFN) type I pathway) (Torralba et al., 2018). Similarly, EVs derived from macrophages infected with *Mycobacterium bovis* (bacillus Calmette-Guérin) stimulate the activation and proliferation of T-cells and IFN-γ production (Giri et al., 2008). It is now thought that many fungal pathogens release EVs that target these mechanisms to regulate virulence, in part, by controlling the host immune system.

The first extensive study of fungal EVs was conducted in 2007 using *C. neoformans*, an opportunistic fungal pathogen that is responsible for causing cryptococcosis, an infectious disease characterized by the fungal colonization of the respiratory system and dissemination to

the central nervous system in either immunocompromised or immunocompetent hosts (Perfect et al., 2014). Through sterol analysis, it was shown that the lipid bilayer of *C. neoformans* EVs was primarily enriched in ergosterol, phosphatidylcholine (PC) and virulent factors glycosphingolipid glucosylceramide (GlcCer) and glucuronoxylomannan (GXM) (Chang et al., 1998; Chang et al., 1999; Ritterhaus et al., 2006; Yoneda et al., 2006; Rodrigues et al., 2007; Oliveira et al., 2009; Nimrichter et al., 2011). Supporting evidence showed *C. neoformans*-derived EVs increased surface expression of immune cell adhesion receptor CD44 upon interaction with human brain microvascular endothelial cells (Huang et al., 2012). *Cryptococcus gattii*, also a causative agent of human cryptococcol disease, releases EVs which seem to mediate a 'division of labour' mechanism which pertains to coordination between fungal cells to enhance dissemination within host macrophage cells (Bielska et al., 2018).

When internalized by bone marrow–derived murine macrophages or dendritic cells, EVs secreted from the human commensal fungus *C. albicans* stimulate NO production in a dose-dependent manner (Zarnowski et al., 2018). Prolonged incubation of host cells with these EVs seems to drive production of distinct cytokine profiles: RAW 264.7 macrophages exposed to these EVs showed low production of IL-10 and TGF-β and elevated IL-12 production, whereas bone marrow–derived murine macrophages exhibit increased levels of IL-10, IL-12p40 and TNF-α (Vargas et al., 2015). Together, these results suggested that EVs may contribute to *C. albicans* infection by modulating host immune cell function.

EVs collected from *Paracoccidioides brasiliensis* (the fungal pathogen that causes paracoccidioidomycosis, a systemic mycosis endemic in Latin America), when added to J7774A.1 macrophage cells, drive production of proinflammatory cytokines (NO, IL-12p40, IL-12p70, IL-6, TNF-α) as well as promoting polarization of M2 'non-protective' macrophages to M1 'protective' macrophages. This suggested that, in tandem with differentiation, these EVs stimulate the fungicidal activity of macrophages, a critical aspect of the host defense strategy (da Silva et al., 2016).

Proteomic analyses of EVs isolated from *Histoplasma capsulatum* (the fungal pathogen causative of histoplasmosis, another endemic in developing Latin American countries) revealed enrichment in chaperone-associated proteins, such as Hsp60, which was shown to bind CD18 receptors on the surface of host macrophages (Lysangela et al., 2019). Interestingly, these EVs are highly immunoreactive with sera from patients diagnosed with histoplasmosis (Albuquerque et al., 2008), and when added to bone marrow-derived macrophages, they trigger phagocytic and fungicidal activity exhibited by patient phagocytes, further supporting the pathogenic nature of these EVs and their cargo proteins.

Overall, these and other studies collectively demonstrate that fungal EVs play critical roles in immunomodulation and pathogenecity. However, most aspects of fungal EV biogenesis, release, recognition, uptake, cargo delivery and bioactivity are not understood in molecular detail. Further dissection of yeast EV physiology will inevitably provide further insight into pathogenesis, and possibly lead to development of new strategies for therapies or to control spread of infection.

A

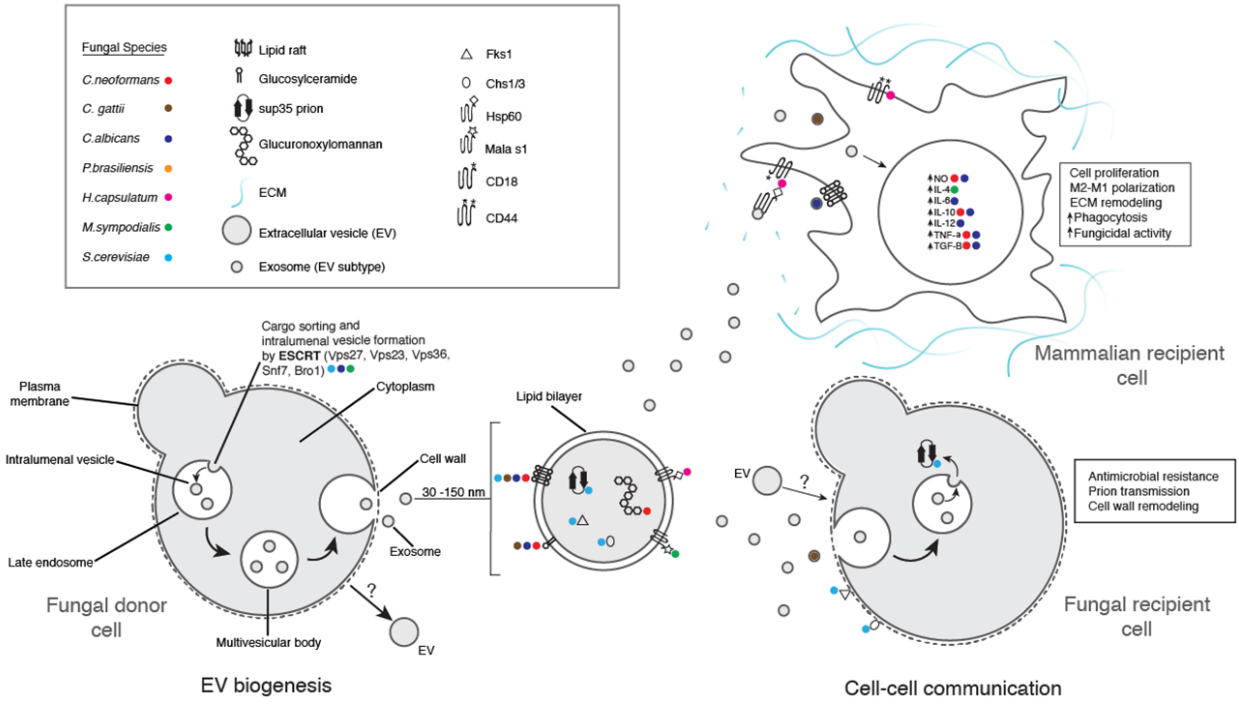

Figure 1. EVs are complex mediators of intercellular communication

(A) Cartoon illustrating both interspecies and intraspecies trafficking of fungal EVs. EV biogenesis occurs through either ESCRT-dependent processes or ESCRT-independent processes (?). Bioactive cargo is sequestered within the lumenal space of vesicles or oriented on the vesicular membrane surface. Cell-cell communication occurs via either internalization of EVs or through direct membrane fusion with the neighboring cell (?) in which the physiological outcome is dependent on EV cargo composition and recipient cell type.

1.4 *Saccharomyces cerevisiae* – model organism to study EV physiology

To better understand fungal EV biology, I reasoned that the non-pathogenic yeast *S. cerevisiae* would serve as an outstanding model to explore this phenomenon in molecular detail. This is because it has been used successfully and extensively to glean mechanistic insight into numerous fundamental cellular processes including key contributors to proteostasis, e.g. the ubiquitin proteasome system, ESCRTs and the canonical heat stress response (Verghese et al., 2012; Feyder et al., 2015). In addition, due to its genetic tractability and low-cost culturing methods, this organism has been used to bio-manufacture recombinant cyclic peptides for therapeutic applications, such as insulin (Bacon et al., 2020). Despite these advances, the contributions of EVs to *S. cerevisiae* physiology remains largely enigmatic.

Although their purpose is largely unexplored, exosomes and other EVs are released by *S. cerevisiae,* a subpopulation of which seems to be made by ESCRTs (Zhao et al., 2019). Limited proteomic studies suggested these EVs contain homologous proteins to those in EVs collected from fungal pathogens or humans, suggesting that key elements of EV biology are conserved (Vallejo et al., 2012; Yang et al., 2017). To date, there are only a few reports of EV function in *S. cerevisiae.* The first suggests a role in cell wall homeostasis (Zhao et al., 2019): two enzymes critical for maintaining cell wall integrity (chitin synthase and 1, 3-β-glucan synthase) present in EV fractions were proposed to help mediate trans-cell wall EV passage after release and were hypothesized to be recognized and taken up by neighboring cells with defective cell walls to promote cell wall biogenesis and survival (Zhao et al., 2019). Low doses of the antifungal drug caspofungin, which targets and weakens cell walls to kill yeast, promotes EV release suggesting *S. cerevisiae* cells may use them for drug–resistance within the population through two mechanisms: by sharing cargo to promote survival, or as an 'EV decoy' that bind and sequester the antifungal agent (Zhao et al., 2019). This finding also demonstrates that *S. cerevisiae* cells share EVs upon stress, a function conserved in mammals (Bewicke-Copley et al., 2017).

Mammalian EVs have been shown to be key players in the intercellular spreading of proteinaceous infectious particles (prions), including those associated with neurodegenerative diseases (Saá et al., 2014; Cerevenakova et al., 2016). Consistent with these findings, *S.*

cerevisiae cells secrete EVs containing the translation termination factor and classic prion protein, Sup35 in its priogenic state (Kabani et al., 2015). These EVs are internalized by recipient cells where they release Sup35 triggering self-sustained aggregation in the cytoplasm, which in turn reduces free pools of Sup35 suppressing translation of downstream transcripts that alter cell metabolism (Liu et al., 2016; Wickner, 2016). To prevent toxic aggregation of Sup35 or to revert cells to their original metabolic state, it was shown that protein chaperones involved in the canonical heat stress response, such as ribosome-associated Hsp70s, bind to and dissolve prion protein aggregates (Chernoff et al., 1999). In support, elevated expression of other heat shock proteins (e.g. Hsp40, Hsp90 and Hsp104) prevented Sup35 prion aggregate formation. On the contrary, absence of these protein chaperones lead to persistent protein misfolding and further imbalance in the cell's functional proteome (Wickner, 2016). Interestingly, these protein chaperones are some of the most abundant cargos enriched in EVs across phyla (De Maio and Vazquez, 2013). However, their roles in prion handling or proteotoxicity by EVs have not been explored in any detail in yeast or mammalian cells. To address this, I hypothesize that perhaps EVs are critical mediators of proteostasis in *S. cerevisiae* populations (**Figure 2**).

1.5 Thesis summary

To test this central hypothesis and better establish *S. cerevisiae* as a model to study EV biology, I first developed and optimized methods for (1) isolating EVs released from yeast in liquid culture under acute stress using ultracentrifugation or filtration, (2) conditioning *S. cerevisiae* cells to heat stress (that induces proteotoxicity) under conditions that better mimic nature and facilitates efficient intercellular communication using a simple colorimetric assay to assess cell viability, and (3) tracking yeast EVs using GFP tagged to Bro1, the presumed ortholog of ALIX, an established marker of mammalian EVs, using fluorometry and fluorescence microscopy.

With new methods in hand, I show that subjecting yeast cells to mild heat stress (42˚C, 30 minutes) is sufficient to protect them from subsequent application of a stronger lethal heat stress. During the conditioning period, I find that cells readily release (and take up) Bro1-GFP positive particles, which I isolated from the extracellular medium. Analysis of these Bro1-GFP positive fractions by quasielastic light scattering (QELS) and atomic force microscopy (AFM) show that they contain nanosized vesicles with diameters averaging 110 nm, characteristic of exosomes. Adding these isolated exosomes to naïve, untreated yeast cells confers protection from lethal heat stress, in a dose-dependent manner, confirming involvement in this response.

Repeating this experiment with recipient cells lacking *END3* abolished protection suggesting that uptake of EVs by endocytosis is necessary. Adding EVs collected during osmotic stress did not protect wild-type cells against lethal heat stress, suggesting cells release different EV populations tailored to unique stress responses. In support, proteomic analysis of these two EV populations revealed different protein content. Notably, two key protein chaperones, Ssa2 and Hsc82, seemed to be enriched in EVs isolated only during heat stress. When I collected EVs from cells missing *HSC82* or *SSA2*, I found that they no longer conferred protection against heat stress when added to wild-type cells, indicating that they likely contribute to this response.

In all, I conclude that *S. cerevisiae* seems to share EVs containing protein chaperones to protect against proteotoxicity triggered by heat stress. I speculate that this may represent an altruistic mechanism for population survival, and discuss how this process contributes to intercellular prion spread. Finally, this work helps establish *S. cerevisiae* as a model to better understand the roles of EVs in proteostasis, and the underlying mechanisms responsible for fungal EV biology applicable to infectious disease.

A

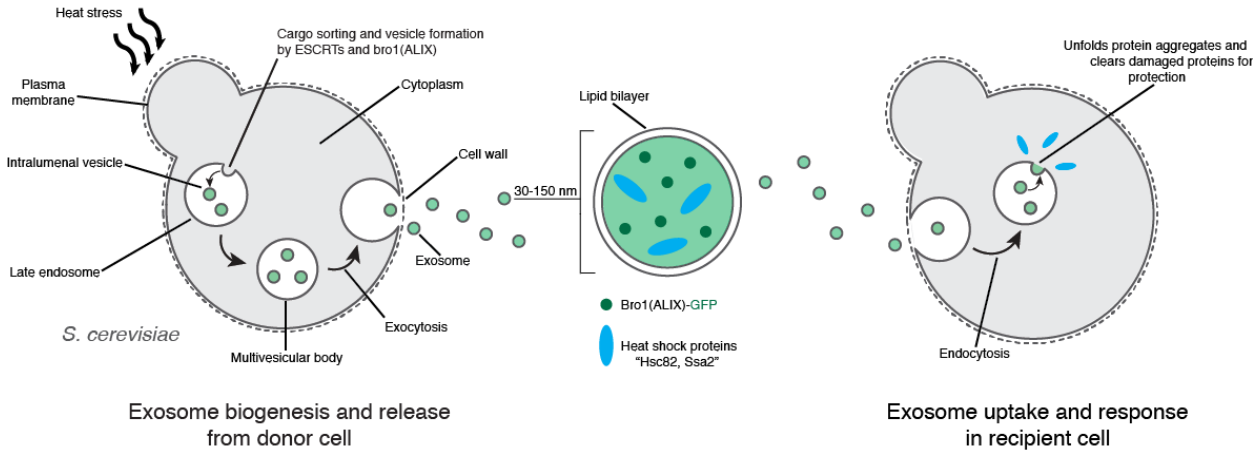

Figure 2. EVs confer protection against lethal heat stress

(A) Working model showing cells subjected to heat stress selectively sorting heat shock proteins into the lumen of intralumenal vesicles (ILVs); an endosomal sorting complex required for transport (ESCRT) driven process along with accessory protein Bro1 (yeast ALIX homolog) – an exosomal biomarker, and the subsequent formation of membrane bound endocytic compartments to which sequester these ILVs – referred to as multivesicular bodies (MVBs). MVBs then undergo fusion with the plasma membrane in which ILVs are released into the extracellular milieu; it is at this stage where ILVs are recognized as exosomes. These exosomes shuttle HSPs to adjacent recipient cells and following endocytosis, release their contents into the cytosol of the recipient cell and promote a pro-survival response.

Chapter 2: Materials and Methods

2.1 Yeast strains and reagents

All *Saccharomyces cerevisiae* strains used in this study are listed in Table 1. Reagents for yeast growth, EV isolation and imaging or biochemical assays were purchased from Thermo Scientific, BioShop Canada Inc., Invitrogen and Sigma-Aldrich.

2.2 EV isolation by ultracentrifugation

In brief, yeast strains were grown for 8 hours at 30 ˚C in 15 mL of yeast peptone dextrose (YPD) medium. The OD_{600nm}/mL was measured and approximately 0.5 ml of pre-culture was added to 1 L YPD medium, which was then incubated for 17 hours at 30 ˚C bringing the final culture OD_{600nm}/ml to ~ 6. Yeast cells were harvested at 3500×g for 10 minutes and the pellet was subjected to mild, sublethal heat stress, which includes incubation at 42 ˚C for 15 minutes, resuspension in 30 mL of phosphate buffered saline (PBS, pH 7.4), and incubation at 42 ˚C for an additional 15 minutes. The cell suspension was then centrifuged at 5,000×g for 15 minutes at 4 ˚C, and the supernatant (containing the extracellular medium) was collected and then centrifuged at 15,000×g for 15 minutes at 4 ˚C to clear it of cellular debris. The supernatant was then filtered (0.22 μm pore size; Corning Inc.) and centrifuged at 100,000×g for 60 minutes at 4 ˚C to sediment EVs. The pellet was resuspended in 100 μl pre-cooled PBS (4 ˚C) and stored on ice prior to further characterization. Protein concentration of EV fractions was determined by Bradford assay, using bovine serum albumin (BSA) to generate standard curves and absorbance was measured at 595nm using a multimode plate reader (Synergy H1, Biotek).

2.3 EV isolation by polyethylene glycol (PEG) - based precipitation

Yeast cells were grown, harvested, and subjected to mild heat stress, and the extracellular medium was collected and filtered as indicated above (for EV isolation by ultracentrifugation). To collect EVs, instead of ultracentrifugation, PEG was added to 30 mL of clarified extracellular medium bringing its final concentration to 10%; the preparation was mixed by inversion, and then incubated overnight at 4 ˚C. Mixture was then centrifuged at 3,200×g for 60 minutes at 4

˚C to sediment EVs. The pellet was resuspended in 100 µl pre-cooled PBS (4 ˚C) and stored on ice prior to further characterization.

2.4 Yeast cell viability assay

Yeast cells were grown in 5 mL synthetic complete (SC) medium for 16 – 18 hours at 30 ˚C, sedimented by centrifugation at 3500×g for 1 minute, and resuspended in 1mL of fresh SC medium. Cell density (OD_{600nm}/mL) was measured, cultures were back-diluted to OD = 20 using fresh SC medium to a final volume of 3 mL, and then incubated at 30 ˚C (CTL) or 42 ˚C (sublethal heat stress) for 30 minutes. During this time, some yeast cell cultures were treated with 1 µg of EVs isolated from a separate yeast culture (containing "donor" cells) as described above. Cultures were then subjected to lethal heat stress (50 ˚C, 30 minutes), cells were sedimented, washed once with SC medium, and resuspended in 100 µL of SC medium prior to addition of 100 µL 0.1% (w/v) methylene blue solution. After incubation for 5 minutes at room temperature, cells were transferred to glass coverslips and imaged under ambient light using a Nikon Eclipse TiE inverted epifluorescence microscope equipped with a 40 × objective lens (Nikon CFI Plan Apo Lambda 0.95 NA), DIC optics, and a color CMOS digital camera (Nikon DsRi2, 4908 × 3264 pixels). Dead methylene blue positive (MB+) and live unstained cells were counted manually using ImageJ software to calculate culture viability. At least three biological replicates (separate yeast cultures on different days) were conducted, and > 200 cells were analyzed using > 5 micrographs for each condition.

2.5 Live cell fluorescence microscopy

To assess EV secretion, live yeast cells were stained with FM4-64 to label vacuole membranes using a pulse-chase method described previously (Brett et al., 2008). Cells were incubated for 1 hour at 30 ˚C in YPD medium containing 3 µM FM4-64 and then sedimented by centrifugation at 3500×g for 1 minute. The cell pellet was washed with 1 mL PBS, and then incubated in the absence (CTL) or presence of sublethal heat stress (42 ˚C for 30 minutes). The pellet was resuspended in 100 µL PBS and imaged using a Nikon Eclipse TiE inverted microscope equipped with a motorized TIRF (Total Internal Reflection Fluorescence)

illumination unit, Photometrics Evolve 512 EMCCD (Electron Multiplying Charge Coupled Device) camera, Nikon CFI ApoTIRF 1.49 NA × 100 objective lens, and 488 nm or 561 nm 50 mW solidstate lasers operated with Nikon Elements software. Cross sectional images were recorded 1 μm into the sample. At least three biological replicates were conducted, and > 300 cells were analyzed using > 10 micrographs for each condition.

For EV uptake, yeast cells were grown in 5 mL synthetic complete (SC) medium for 16 – 18 hours at 30 ˚C, sedimented by centrifugation at 3500×g for 1 minute, and resuspended in 1 mL of fresh SC medium. Cell density (OD_{600nm}/mL) was measured, cultures were back-diluted to OD = 0.1 using fresh SC medium to a final volume of 1 mL (Zhao et al., 2019). Cells were then resuspended in calcofluor white (Fluorescent Brightener 28-Sigma, F3543) solution (1 mg of calcofluor white dissolved in 1 mL of 100 mM Tris, pH 9.5, filter sterilized) and incubated at room temperature for 20 minutes in order to label cell wall. Cell suspension was washed in 1 mL SC and resuspended in 80 uL of SC. EV fractions were diluted to a concentration of 0.1 μg/μL in pre-cooled PBS. 10 μL of diluted cells, 10 μL of diluted EV fractions and 80 μL of SC incubated for 30 minutes in the absence (CTL) or presence of sublethal heat stress treatment at 42 ˚C for 30 minutes and imaged as above. At least three biological replicates were conducted, and > 100 cells were analyzed using > 10 micrographs for each condition.

2.6 EV characterization by fluorometry and quasi-elastic dynamic light scattering (QELS)

GFP fluorescence (λ_{ex} = 488 nm; λ_{em} = 510 nm) was measured after transferring 100 μL of EV samples to a black 96-well conical-bottom microtiter plate using a fluorescence multimode plate reader (Synergy H1, Biotek). To measure size by QELS, EV fractions were diluted (1:5) in PBS to reach a final volume of 100 μL and loaded into a QS 1.50 mm quartz cuvette. Using a DynaPro-Microsampler (Wyatt Technology), particle size analysis was conducted at 4 °C and laser power was manually adjusted to acquire a count rate of > 1 million. Size distribution profiles were examined using Dynamics 6.7.7.9 analysis. At least three biological replicates were conducted and the average diameter was measured by 100 consecutive acquisitions per sample.

2.7 Atomic force microscopy (AFM)

EVs isolated from yeast cells expressing Bro1-GFP were diluted (1:5) in PBS to a final volume of 100 µL, added to freshly cleaved mica sheet (Ted Pella Inc), and airdried. 1% triton (Anapoe) X-100 (Anatrace) was added to some samples to help determine if observed particles were membrane-bound. Using a multimode AFM (Veeco Metrology Instruments) configured with a 10X objective lens (Nikon), charged-coupled device (CCD) camera and scanning probe controller (Nanoscope 3a with a Quadrex Extender), images of samples were then captured with Nanoscope v5.30 acquisition software. Specifically, samples were scanned in air by tapping mode AFM using a silicon AFM probe (Tap300AI-G) with a resonant frequency of 300 kHz and force constant of 40 N/m (Budget Sensors). Scanning rate was fixed at 1.00 Hz, and amplitude set–point was adjusted to 75% of the pop-off voltage for medium tapping. Image analysis was conducted using NanoScope v1.5 analysis software. Each sample was imaged at least three times (technical replicates) and at least three EV samples from different yeast cultures (biological replicates) were examined.

2.8 Liquid chromatography-tandem mass spectrometry (LC-MS/MS)

For proteomic analysis by LS-MS/MS, EV fractions (2 µg) isolated from yeast expressing Bro1-GFP during sublethal heat stress or osmotic stress were resolved by SDS-PAGE, gels were stained with Coomassie Brilliant Blue R-250 (BioShop) to visualize protein samples that were excised. Gel pieces were then added to 200 µL 50 mM NH_4HCO_3 containing 10 mM dithiothreitol (DTT; a reducing agent) and incubated for 30 minutes at room temperature. 200 µL 50 mM NH_4HCO_3 containing 50 mM iodoacetamide (for alkylation) was added, and the sample was incubated for 30 minutes at room temperature. Reduced and alkylated gel pieces were then washed at room temperature with 50 mM NH_4HCO_3 for 15 minutes, 25 mM NH_4HCO_3 containing 5% acetonitrile (ACN) for 15 minutes, 25mM NH_4HCO_3 containing 50% ACN for 30 minutes (twice), and 100% ACN for 10 minutes. Gel pieces were then dried at 43 °C by Speed Vac (Savant) and rehydrated in 25 mM NH_4HCO_3 containing porcine pancreas trypsin (Sigma Aldrich) for 12 – 14 hours at 30 ˚C. Digested peptides were then extracted by incubating samples with 60% ACN containing 0.5% formic acid. Extracted peptides were dried at 43 ˚C by Speed

Vac and stored at -20 ˚C. Samples were resuspended in 10 µL 5% methanol containing 0.1% trifluoroacetic acid (TFA) and analyzed by LC-MS/MS using a Thermo LTQ Orbitrap Velos mass spectrometer with a nano-spray ion source confiigured with Thermo EASY nLC II liquid chromatography system at the Centre for Biological Applications of Mass Spectrometry (CBAMS) at Concordia University. At least two biological replicates were conducted per condition.

2.9 Data analysis and presentation

Micrographs and GFP fluorescence intensity profiles were processed using ImageJ software and Adobe Photoshop CC.

GFP intensity measurements shown in Fig. 3C were generated using the ImageJ Cell Counter plugin. Micrographs were quantified by calculating relative intracellular GFP fluorescence. Prior to quantification, background fluorescence was subtracted and GFP fluorescence intensities were determined using a 4×4 pixel region of interest to measure mean GFP fluorescence of the cells.

GFP location measurements shown in Fig. 5A were generated using the ImageJ Cell Counter plugin. Micrographs were quantified by counting the total number of cells and the number of cells where the GFP fluorescence was detected on the intracellular puncta.

For cell viability assays, proportion of positively MB stained cells (dead) in Figs. 3AB, 6A-E, 7D, 9B and S2A were manually counted using the ImageJ Cell Counter plugin. Micrographs were quantified by counting the total number of cells and the number of cells stained with MB (dead).

Mass spectrometry data was analyzed using Proteome Discoverer 2.4 software (Thermo Scientific). Of the total 543 proteins identified in this study, acquired data was compared to Vesiclepedia (Version 3.1, 2017) to assess overlap of previously conducted EV protein enrichment analyses experiments. Venn diagrams were generated using functional enrichment software FunRich (Version 3.1.3, 2020). Protein abundances were calculated and normalized by

consensus workflow nodes: precursor ions quantifier node and reporter ions quantifier node as programmed in the proteome software.

Data are reported as mean ± S.E.M. Comparisons were calculated using Student two-tailed t-test; *P*- values are indicated and $P < 0.05$ suggests significant differences. An experiment is defined as a sample prepared from a separate yeast culture on different days. Micrographs were processed using ImageJ and Adobe Photoshop CC software.

Table 1. *S. cerevisiae* strains used in this study

Strain	Genotype	Source
BY4741	*MATα his3-Δ1 leu2-Δ0 met15-Δ0 ura3-Δ0*	Huh et al., 2003
Bro1-GFP	BY4741, *Bro1-GFP:: His3MX*	This study
chs1Δ	BY4741, *chs1:: KanMX*	This study
end3Δ	BY4741, *end3Δ:: KanMX*	This study
hsc82Δ	BY4741, *hsc82Δ:: KanMX*	This study
ssa2Δ	BY4741, *ssa2Δ:: KanMX*	This study

Chapter 3: Results

3.1 EVs are released from *S. cerevisiae* when conditioned to heat stress

Previous reports demonstrated that fungal EV shuttling is increased in densely grown cell cultures (Rodrigues et al., 2019). Moreover, EVs derived from heat stressed epithelial cells enhanced the ability of naïve (unstressed) recipient cells to survive subsequent heat stress treatment suggesting EVs possess prosurvival information (Bewicke-Copley et al., 2017). Given that EV intercellular communication is evolutionary conserved, I first tested the hypothesis that growing *S. cerevisiae* cell cultures in high density and subjecting these cells to sublethal heat stress would enhance EV-mediated communication which would assist in maintaining cell viability. As predicted, after 30 minutes at 42 ˚C (sublethal) high density cell cultures (6×10^8 cells/mL), cell viability did not significantly differ from cell cultures incubated for 30 minutes at 30˚C (control temperature) (**Figure 3A and B**). To begin testing the central model (**Figure 2**), I hypothesized donor yeast cells under milder (sublethal) heat stress release EVs and enable recipient cells to better mitigate the deleterious effects induced by subsequent extreme (lethal) heat stress. To test this, high density cell cultures were subjected to sublethal heat stress for 30 minutes followed by another 30 minute incubation period at 50 ˚C (lethal). I found that cell viability significantly differed from cell cultures incubated for 30 minutes at 50 ˚C (lethal) alone (**Figure 3A and B**). These data suggested the involvement of a protective mechanism, however, it still remained unclear if EV spread was the direct contributor of this effect.

Because mammalian EVs have been implicated in proteotoxicity in heat stress conditions (Asai et al., 2015; Bewicke-Copley et al., 2017), we next tested the hypothesis that *S. cerevisiae* release EVs during mild, sublethal heat stress. Because ALIX is considered an established biomarker of EVs by the research community (Théry et al., 2018), I used its yeast ortholog, Bro1, tagged to GFP to track EVs in populations of *S. cerevisiae*. Bro1-GFP is present at MVBs within cells, where it contributes to ILV (exosome) biogenesis, and gets entrapped in newly formed EVs, allowing us to follow them from synthesis within donor cells, to release into the extracellular medium, to consumption after uptake by recipient cells.

Using highly inclined laminated optical sheet (HILO) fluorescence microscopy, I first imaged Bro1-GFP within live donor yeast cells (**Figure 3C**). As expected, Bro1-GFP localized to multiple puncta near vacuoles (stained with FM4-64), reminiscent of MVBs filled with newly formed EVs (Karim et al., 2018). Next, I subjected cells to sublethal heat stress (42 ˚C) and found fewer puncta and less Bro1-GFP fluorescence within cells after 30 minutes (**Figure 3C and D**). Loss of Bro1-GFP signal within cells suggested that either the protein was degraded or MVBs fused with the plasma membrane releasing EVs containing Bro1-GFP.

To explore the latter possibility, I used differential ultracentrifugation to isolate EVs from the extracellular medium collected from yeast cultures. Originally, I attempted to use existing protocols (Rodrigues et al., 2019), but EV yields were incredibly low preventing further characterization. Moreover, previous studies only collected EVs released from (unstressed) cells during culture growth for 16 – 41 hours, which if replicated would not render EVs exclusively released during stress. Thus, after substantial trial and error, I optimized a new method to isolate EVs released only during 30 minutes, with or without sublethal heat stress, and at yields sufficient for characterization (**Figure 3E**). After collecting EV fractions from stressed and unstressed cells, I detected significantly higher protein concentration (**Figure 3F**) and higher Bro1-GFP fluorescence (**Figure 3G**) when heat stress was applied, as determined by Bradford assay and fluorometry, respectively. This suggested that under sublethal heat stress, Bro1-GFP labeled EVs are released from donor cells into the extracellular medium.

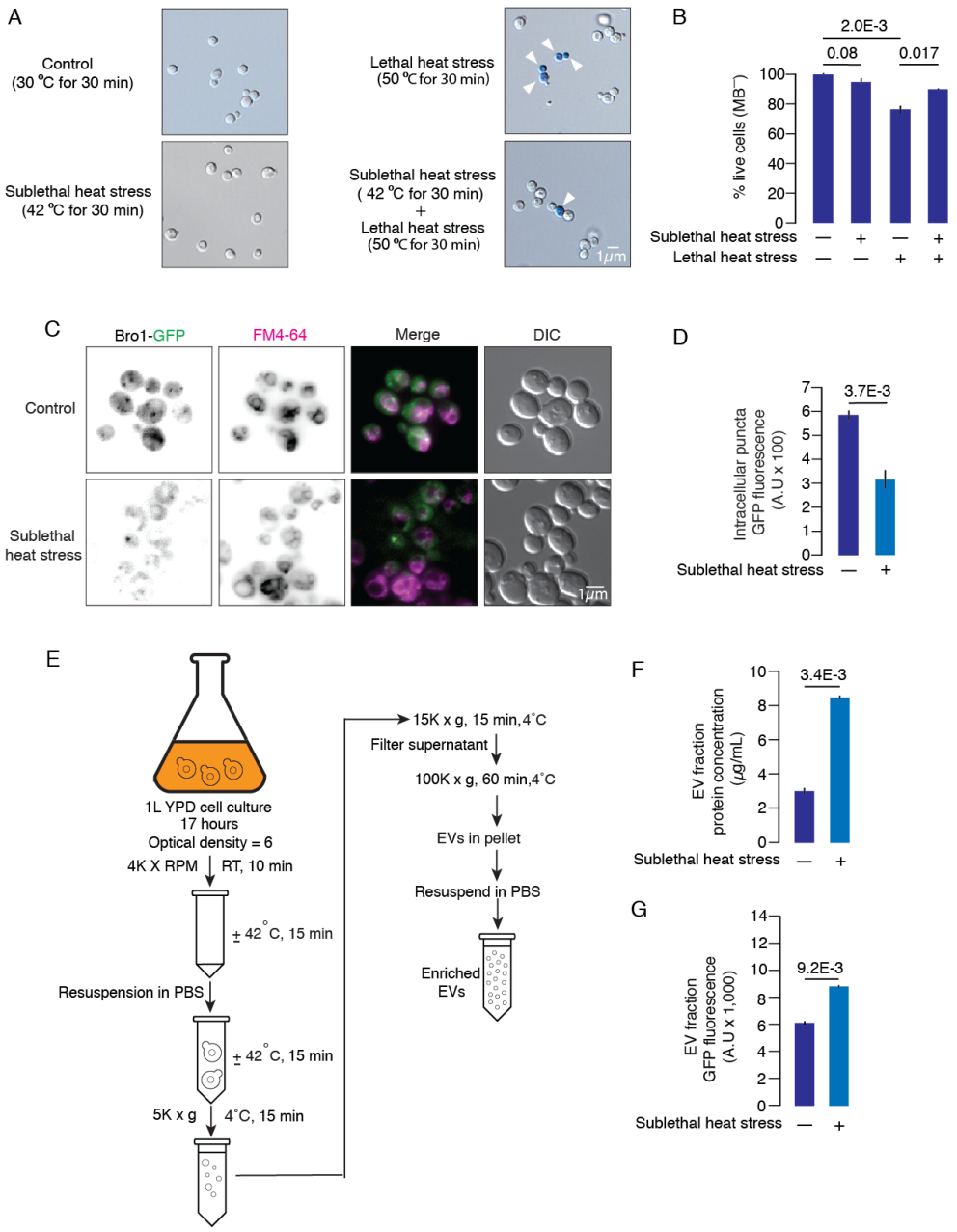

Figure 3. Sublethal heat stress stimulates Bro1-GFP release from live yeast cells

(A) Light micrographs of wild-type cells stained with methylene blue to assess cell death. A sublethal heat stress preconditioning treatment involved a 30 minute exposure at 42 ˚C, followed by a 30 minute recovery growth period at 30 ˚C. Lethal heat stress (50 ˚C for 30 minutes) was applied after the preconditioning period. **(B)** Using micrographic shown in **A**, the proportion of methylene blue-negative cells (viable) from all cells imaged was calculated (n = 3). **(C)**

Fluorescence micrographs of live wild-type yeast cells expressing GFP tagged Bro1 stained with FM4-64 to label vacuole membranes after treatment without (control) or with sublethal heat stress. **(D)** Using micrographic data shown in **C,** total cell GFP fluorescence was measured ($n \geq 120$ cells per condition). **(E)** Schematic of EV isolation protocol. **(F, G)** EVs isolated after 30 minutes with or without heat stress were analyzed by Bradford assay (to assess total protein concentration, F) and fluorometry (to assess Bro1-GFP levels, G) ($n = 3$). Mean ± S.E.M. and *P*-values from two-tailed Student t-tests are shown. Scale bars, 1 μm.

3.2 Dimensional characterization and visualization of yeast EV fractions

EVs are a heterogeneous population of membrane-bound particles released from eukaryotic cells, which are classified primarily by size (Wu et al., 2017). With this in mind, I aimed to confirm that extracellular fractions collected from *S. cerevisiae* during heat stress contained membrane-bound vesicles, and that they are exosomes based on size, as inferred by the presence of Bro1-GFP. I first used atomic force microscopy (AFM) to visualize EV fractions, as individual exosomes (30 – 150 nm diameter) are too small to be discerned by light microscopy, and AFM was successfully used to determine size and composition of EV populations derived from human cells (Sharma et al., 2018). I found that fractions collected under heat stress showed an abundance of circular features 30 – 80 nm in diameter (**Figure 4A**). I next treated samples with the detergent Triton X–100 (1 %) to dissolve lipid membranes, and predicted to observe no features if they represent EVs. As expected, no discernible circular features were observed in the presence of detergent (**Figure 4B**), suggesting that they represent membrane-bound EVs in the size range of exosomes.

Isolation by ultracentrifugation may crush or fragment vesicles, possibly leading to inaccurate assessments of structure and size (Konoshenko et al., 2018). Thus, I repeated this experiment using an alternative method for EV isolation that involved gentle precipitation with 10 % PEG, avoiding exposure of samples to potentially damaging centrifugal force and reducing possible contamination by soluble protein complexes (Rider et al., 2016). Upon imaging these samples by AFM, I observed similar, but less abundant, circular features that disappear upon

Triton X-100 treatment (**Figure S1)**. This suggested the presence of EVs in the extracellular medium collected from yeast exposed to heat stress.

Although AFM is an accepted method to visualize individual nano-sized vesicles, a drawback is that sample fixation requires dehydration, which effectively reduces vesicle volume resulting in an underestimate of diameter (Skliar et al., 2019). Thus, to better estimate their size, I instead measured diameters of the EV population in solution, immediately after isolation, using quasi-elastic light scattering (QELS). I observed particles with diameters from 100 to 130 nm in diameter when examining samples prepared by ultracentrifugation (**Figure 4C**) or PEG sedimentation (**Figure S1**). As expected, these measurements were larger than estimates provided by AFM, and a more accurate measure of EV size, but both methods rendered values within the size range (30 – 150 nm diameter) that defines exosomes, confirming that they are the dominant subpopulation of EVs released from yeast cells during heat stress.

A

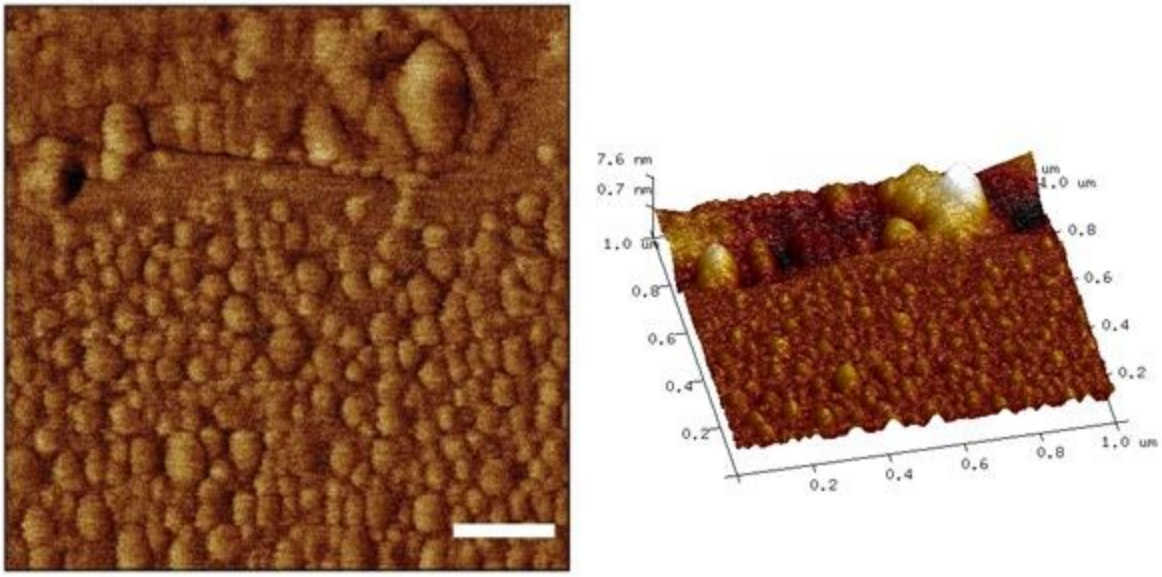
7.6 nm
0.7 nm
1.0 um
0.8
0.6
0.4
0.2
0.2
0.4
0.6
0.8
1.0 um

B

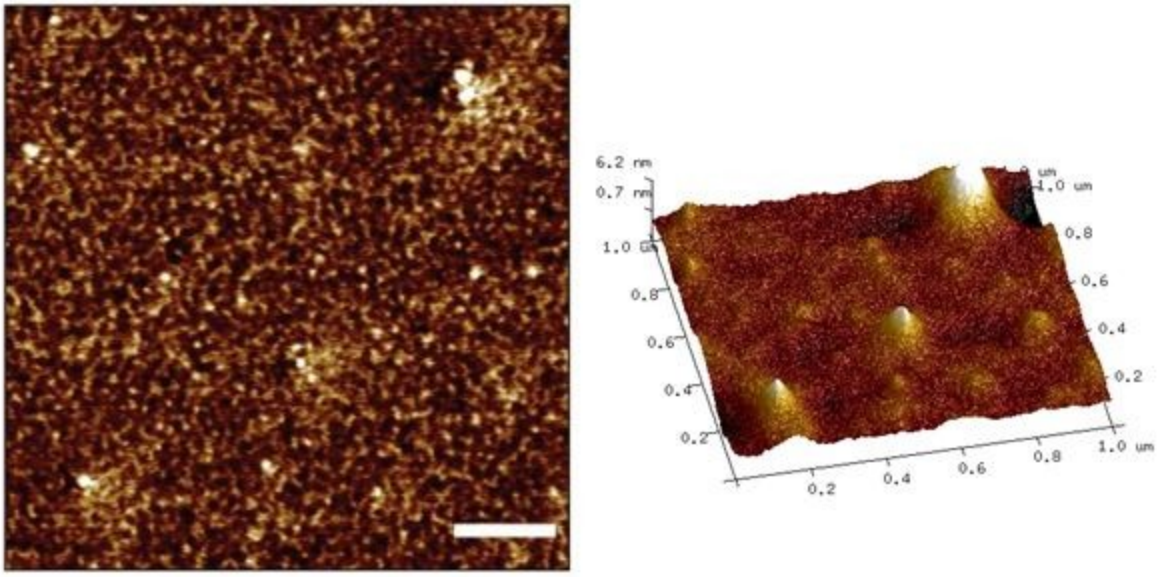
6.2 nm
0.7 nm
1.0 um
0.8
0.6
0.4
0.2
0.2
0.4
0.6
0.8
1.0 um

C

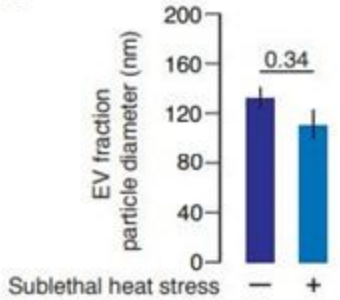
200
160
120
80
40
0
EV fraction particle diameter (nm)
0.34
Sublethal heat stress
—
+

Figure 4. Visualization and particle size analysis of EV samples isolated from yeast during sublethal heat stress

(A, B) Phase (left) and topographical mapping (right) images of EV fractions isolated by ultracentrifugation from yeast cultures during sublethal heat stress in the absence (A) or presence (B) of Triton X-100 acquired using AFM. Examples of 3 independent experiments are shown. **(C)** QELS analysis of EV fractions collected from yeast cells expressing Bro1-GFP after 30 minutes at 30 ˚C (–) or 42 ˚C (+ sublethal heat stress) (n = 3). Mean ± S.E.M and *P*-value from Student's t-test are shown. Scale bars, 200 nm, 1 μm × 1 μm scan.

3.3 EVs are readily endocytosed by *S. cerevisiae* during heat stress

Although it is now evident that particles resembling EVs are released by yeast cells during sublethal heat stress, it remains unclear if or how they may contribute to the observed protective response. For example, as originally proposed when EVs were discovered (Pan et al., 1983), yeast cells may sequester proteins and other biomolecules susceptible to becoming toxic under heat stress within EVs and release them as "trash bags" to improve odds of survival. Alternatively, EVs may be recognized by recipient cells and deliver their bioactive cargo to trigger a protective response, i.e. mediate intercellular communication. If so, cargo delivery from the lumen of EVs to the cytoplasm of recipient cells is thought to occur by either direct EV-plasma membrane fusion, or EV uptake by endocytosis whereby sequestered EVs supposedly undergo back–fusion with endosome membranes within cells (Hessvik et al., 2018; Maas et al., 2018).

To determine whether these EVs mediate intercellular communication, I first assessed whether they are internalized and sequestered within endosomes of recipient cells. To do so, I added Bro1-GFP labeled EVs isolated from donor cells during heat stress to live naïve (unstressed), GFP-free recipient cells in culture and imaged them using HILO fluorescence microscopy. After 30 minutes at 30 ˚C (control temperature), I observed Bro1-GFP puncta only within live recipient cells treated with EVs, whose outer perimeters were stained with calcofluor white that selectively labels the cell wall (**Figure 5A**). This result suggested uptake of EVs

within endosomes, where they accumulate permitting visualization by fluorescence microscopy (as reported by others; Toribio et al., 2019). It also supported the notion that EVs can pass through large pores within the glycoprotein matrix that forms the yeast cell wall (see Pereira and Geibel, 1999; Pillet et al., 2014; Casadevall et al., 2015), supported by my observation that EVs are also released from intact yeast cells into the surrounding environment, which again requires passage through the cell wall but in the opposite direction (**Figure 3**).

Because subtlethal heat stress stimulates EV release, I hypothesized that EV uptake is also enhanced to support efficient intercellular communication. To test this hypothesis, recipient cell cultures were subjected to sublethal heat stress (42 ˚C) following EV treatment (**Figure 5A**). As expected, I found that more recipient cells in the population contained Bro1-GFP and these cells seemed to contain more Bro1-GFP puncta (**Figure 5B**). Thus, I concluded that both EV release and uptake are stimulated during sublethal heat stress, suggesting they mediate intercellular communication.

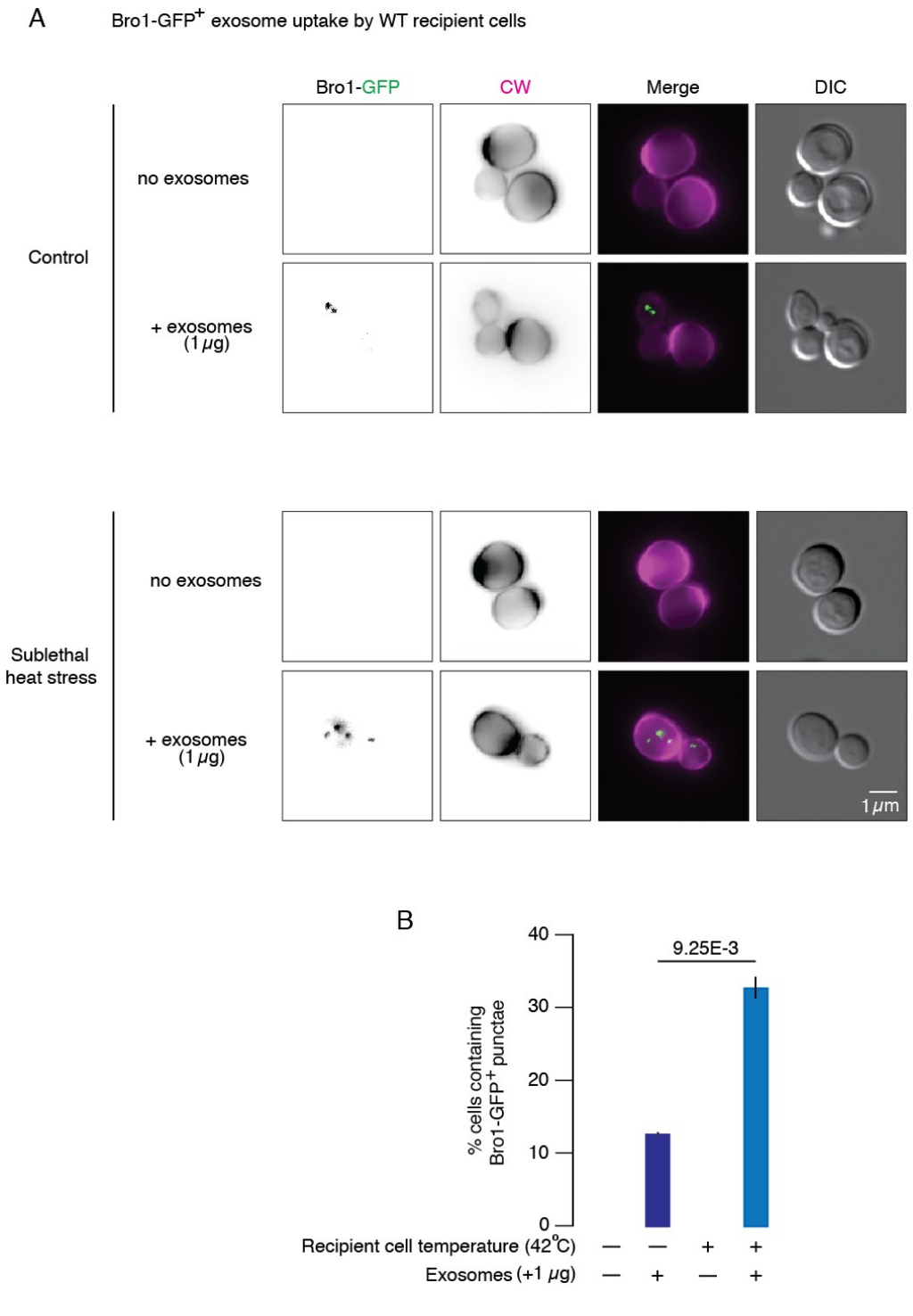
A
Bro1-GFP+ exosome uptake by WT recipient cells
Bro1-GFP
CW
Merge
DIC
Control
no exosomes
+ exosomes (1 μg)
Sublethal heat stress
no exosomes
+ exosomes (1 μg)
1 μm
B
9.25E-3
% cells containing Bro1-GFP+ punctae
40
30
20
10
0
Recipient cell temperature (42°C) — — + +
Exosomes (+1 μg) — + — +

Figure 5. Sublethal heat stress stimulates EV uptake by recipient cells

(A) Fluorescence micrographs of live non-GFP expressing WT cells stained with calcofluor white to label cell wall and treated with Bro1-GFP^{+} labelled EVs derived from stressed cultures under low cell density conditions in absence (CTL) or presence of sublethal heat stress. **(B)** Using micrographic data shown in **A** the proportion of cells with GFP^{+} puncta was quantified (n = 3). Mean ± S.E.M and *P*-value from two-tailed Student t-test shown. Scale bar, 1 μm.

3.4 EVs confer protection against lethal heat stress

After taken up within endosomes by recipient cells, EVs must release their cargo to elicit a response, the end-point of communication. Alternatively, they may be sent to lysosomes (or vacuoles in yeast), the terminal compartment of the endocytic pathway, where they are catabolized and used as a source of nutrients (McNally and Brett, 2017). Thus, it remains unclear if EVs shared during conditioning are simply digested or contribute to a response by recipient cells that specifically protects them from lethal heat stress. To determine if EVs confer heat tolerance, I repeated experiments that assess cell viability after sublethal heat stress (**Figure 3**), except instead of conditioning cells with a brief sublethal heat stress (42 ˚C) for 30 minutes, I added EVs collected from a separate yeast culture, to naïve (unstressed) cells at control temperature (30 ˚C). I predicted that the EVs alone (collected under sublethal heat stress from Bro1-GFP cells) should confer protection if they contribute to this response. As expected, addition of EVs were sufficient to protect naïve cells from lethal heat stress (**Figure 6A**). This effect was dose-dependent showing an equivalent effect to conditioning (by sublethal heat stress) when 1 μg of EVs or more were added (**Figure 6B**). These data demonstrated that intercellular communication by EVs is an important contributor to cell survival upon heat stress.

With this EV bioactivity assay in hand, I next tested the involvement of the cell wall and endocytosis in this response. First, to confirm that the cell wall does not impede communication by EVs, I examined effects of deleting *CHS1*, a gene encoding a chitin synthase required for cell wall biosynthesis (Casadevall et al., 2015), on the ability of EVs to confer protection against heat stress. If the cell wall obstructs EV passage, then *chs1*Δ recipient cells that possess weakened

cell walls should be more accessible to EVs and show a stronger response. However, as predicted, deleting *CHS1* had no effect on cell survival after lethal heat stress, with or without conditioning or treatment with EVs (**Figure 6D**). This finding is consistent with the cell wall allowing free passage of EVs for intercellular communication.

Next, to confirm that endocytosis of EVs contributes to the observed response, I repeated the experiment with recipient cells lacking *END3*, a gene encoding an essential component of the endocytic machinery (Giardina et al., 2014), to impair endocytosis. As predicted, the protective effect observed when adding isolated EVs to naïve *end3*Δ cells was diminished, but not completely abolished (**Figure 6E**). In support, conditioning *end3*Δ cells with sublethal heat stress (without adding purified EVs) showed less protection as compared to wild-type cells (see **Figure 6A**). This result suggested that endocytosis of EVs, presumably needed to deliver their cargo, contributes in part to this protective response, but other mechanisms may be at play (e.g. direct EV-plasma membrane fusion).

A

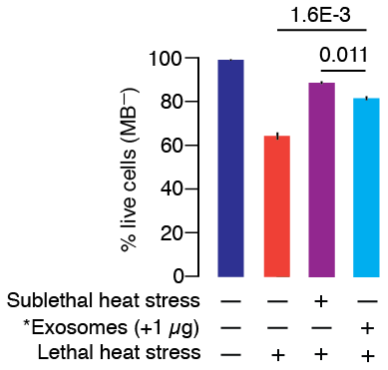
* Exosomes isolated from sublethal heat stressed WT donor cells
1.6E-3
0.011
100
80
60
40
20
0
% live cells (MB⁻)
Sublethal heat stress — — + —
*Exosomes (+1 μg) — — — +
Lethal heat stress — + + +

B

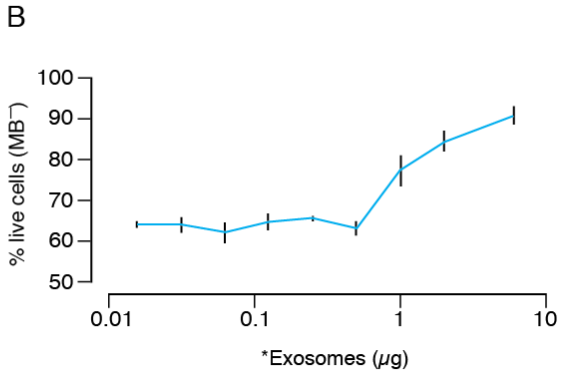
100
90
80
70
60
50
% live cells (MB⁻)
0.01
0.1
1
10
*Exosomes (μg)

C

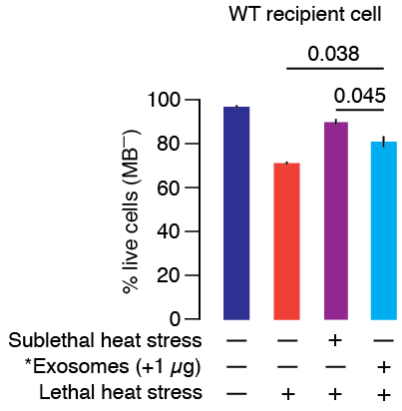
WT recipient cell
0.038
0.045
100
80
60
40
20
0
% live cells (MB⁻)
Sublethal heat stress — — + —
*Exosomes (+1 μg) — — — +
Lethal heat stress — + + +

D

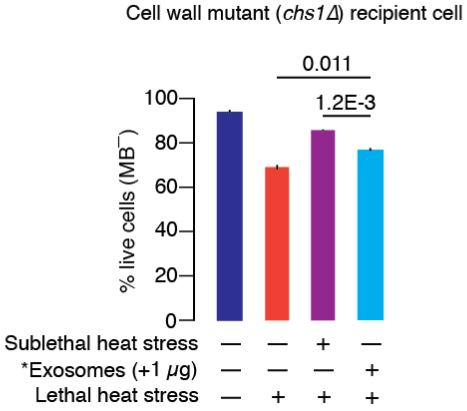
Cell wall mutant (chs1Δ) recipient cell
0.011
1.2E-3
100
80
60
40
20
0
% live cells (MB⁻)
Sublethal heat stress — — + —
*Exosomes (+1 μg) — — — +
Lethal heat stress — + + +

E

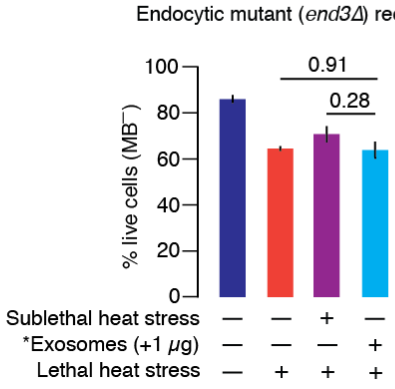
Endocytic mutant (end3Δ) recipient cell
0.91
0.28
100
80
60
40
20
0
% live cells (MB⁻)
Sublethal heat stress — — + —
*Exosomes (+1 μg) — — — +
Lethal heat stress — + + +

Figure 6. EVs protect yeast cells from lethal heat stress

(A) The proportion of methylene blue-negative cells (live) from all cells imaged was determined (n = 3). **(B)** Dose-dependent response curve showing wild-type recipient cells treated with increasing amounts of EVs isolated from donor cells after sublethal heat stress (n = 3). **(C)(D)(E)** Proportion of methylene blue-negative stained WT, cell wall mutant (*chs1*Δ*)* and endocytosis mutant (*end3*Δ) recipient cells treated with EVs derived from derived from WT donor cells subjected to sublethal heat stress (n = 3). Mean ± S.E.M. and *P*-values from two-tailed Student t-tests shown are shown.

3.5 Protection by EVs shared during conditioning is stressor-specific

Currently, it is unclear if *S. cerevisiae* or other fungal cells selectively release different EV populations to mediate specific cellular responses (the favoured view with insufficient supporting evidence), or if they contain a single "universal" EV population that is constitutively biosynthesized and released to ensure survival when confronted with toxic stress. This is because prior to this study, researchers only collected EVs over 16 – 41 hours from unstressed *S. cerevisiae* cells (Liu et al., 2016; Rodrigues et al., 2019; Zhao et al., 2019). These samples likely contain diverse EV populations, given that they are collected during multiple, different stages of culture growth, but also lack any EVs that may be exclusively shared when the cell population is confronted with stress. Rather, herein, I isolated EVs during a short, 30–minute period (unaffected by culture growth) when defined stressors are applied (or not) offering the opportunity to begin to address if EV-mediated communication is stressor-specific.

To do so, I tested if yeast EVs collected under a different stressor confer protection against lethal heat stress. To begin, I tested exposure to hypoosmotic medium (2 % glucose in water; 100 mOsm versus 280 mOsm for PBS used under control and heat stress conditions) for 30 minutes at 30 ˚C. It is worth noting that standard yeast growth medium contains 1 % yeast extract, 2 % peptone and 2 % glucose (250 mOsm). I removed all components except for glucose (the carbon source) to induce hypoosmotic stress, but recognize that all sources of nitrogen are

missing. A similar strategy is sometimes used to study nitrogen starvation, but requires many hours to trigger a cellular response (Johnstone et al., 1977). Rather, I only stress cells for 30 minutes, a period that includes their acute responses to an immediate drop in extracellular osmolarity, but not initiation of known starvation signaling. This stressor was used because it was predicted to drive MVB–plasma membrane fusion, releasing EVs from cells (Rice et al., 2015), or drive cell swelling to trigger cell wall remodeling which may involve signaling by EVs (Zhao et al., 2019).

I first used differential ultracentrifugation to isolate EVs from yeast cells expressing Bro1-GFP exposed to hypoosmotic stress, and found that samples contained significantly higher total protein concentration but lower Bro1-GFP fluorescence as compared to EVs isolated under heat stress (**Figure 7A and B**). QELS analysis showed that EVs collected under either condition had similar mean diameters (**Figure 7C**). However, when I added EVs collected under hypoosmotic stress to naïve recipient cells, I found that they did not confer protection to lethal heat stress (**Figure 7D**), suggesting that different EV populations are released under osmotic or heat stress. If true, and these are separate pools of EVs made or stored within cells, then I hypothesize that the amount of EVs released from a single cell population should be additive when stressors are applied in tandem. As predicted, I found that EV release was additive when collecting EVs from donor cells treated with sublethal heat stress immediately followed by hypoosomotic stress, based on measuring protein concentration and Bro1-GFP fluorescence of EV fractions (**Figure 7A and B**). These important findings support the idea that yeast cells can selectively release unique pools of EVs with different bioactivities depending on stress.

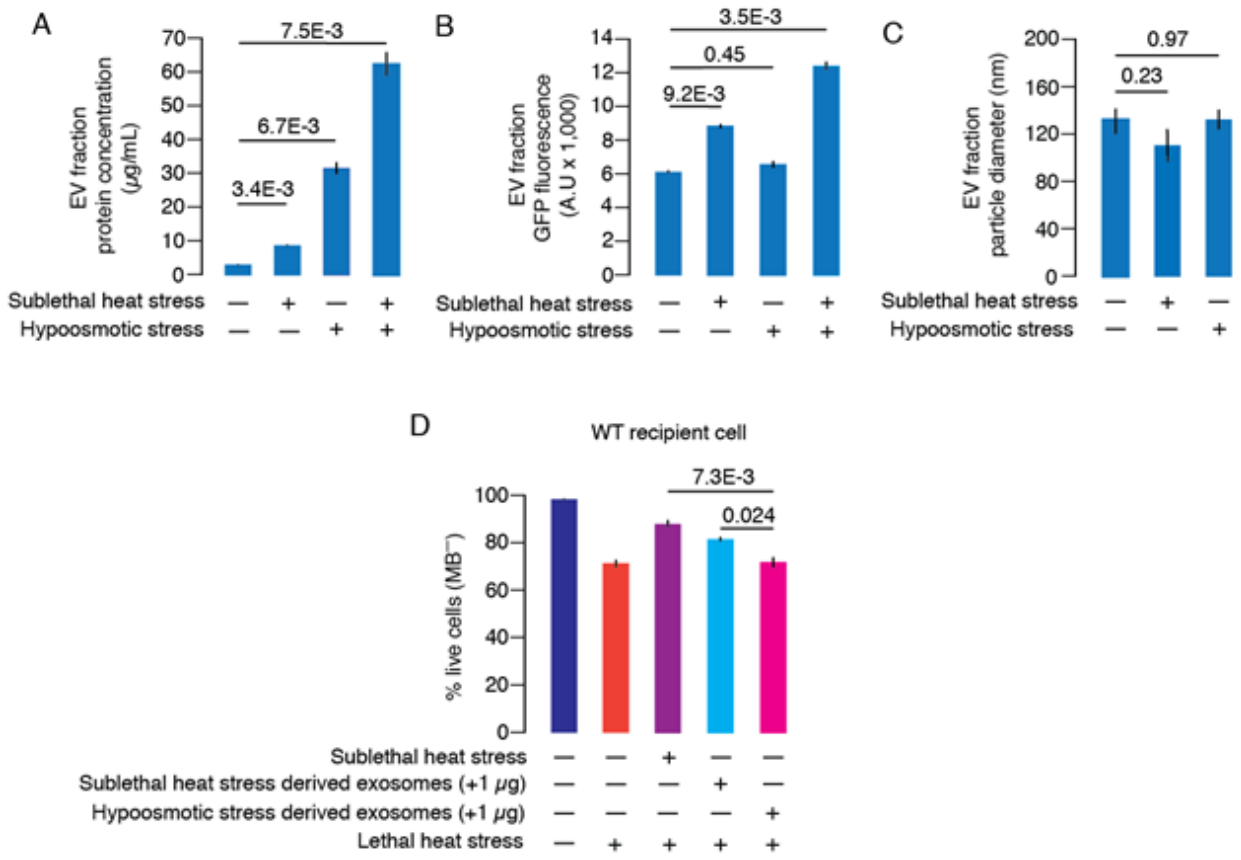

Figure 7. Protective effect of yeast EVs appears to be stressor-specific

(A)(B) EV fraction protein concentration and fluorescence was determined by Bradford protein assays and fluorometry assays, respectively (n = 2). **(C)** Results from QELS analysis are shown, to provide preliminary confirmation of isolated EVs from donor cells subjected to hypoosmotic stress or heat stress (n = 3). **(D)** Proportion of methylene blue-negative stained WT recipient cells treated with EVs derived from hypoosmotically shocked donor cells (n = 3). Mean ± S.E.M. and *P*-values from two-tailed Student t-tests shown are shown.

3.6 Protein chaperones are enriched in EVs released during heat stress

EVs are composed of complex biomolecules (lipids, sugars, proteins, nucleotides) responsible for all aspects of intercellular communication. In theory, these include essential components of basic EV structure and integrity as well as machinery for cell recognition, uptake and membrane fusion for example, presumably found in all EVs. However, different EV populations should also contain unique cargoes (RNAs or proteins) that elicit specific responses by recipient cells.

In an effort to identify cargo proteins within EVs that contribute to protection from lethal heat stress, I conducted proteomic analysis of yeast EV samples by liquid chromatography - tandem mass spectrometry (LC-MS/MS). I decided to analyze EVs collected during either sublethal heat stress or hypoosmotic stress, and compare their proteomes to identify unique or enriched proteins packaged within EVs during heat stress. During heat stress, 402 proteins were identified in released EVs and 435 in EVs during hypoosmotic stress (**Figure 8A**). Of these, 294 were found in both samples, likely representing, in part, common EV machinery. I then compared my dataset to the published proteome of EVs collected from unstimulated *S. cerevisiae* for 16 – 41 hours during culture growth (Oliveria et al., 2010; Zhao et al., 2019; obtained from Vesiclepedia, an online, open-access EV molecular database). When cross-referenced to these 1,268 proteins, I found that EVs isolated in this study shared 284 proteins, 201 of which were identified under all conditions tested, representing 16% of previously documented EV proteins (**Figure 8A**). From this analysis, I also identified 80 proteins uniquely found in EVs isolated during sublethal heat stress (**Figure 8A; Table S2**). Although most showed low-abundance and low-peptide coverage, some proteins represent interesting candidates warranting further investigation in the future, e.g. Hch1, a Hsp90 co-chaperone implicated in protein refolding as part of the canonical heat stress response.

Rather, I focused on the most abundant proteins found in EVs collected during heat stress (**Table S2**). These include enolases Eno1 and Eno2, phosphoglycerate kinase Pgk1, glucan 1, 3-beta-glucosidase Exg1, Hsp70 family ATPase Kar2, as well as four key protein chaperones involved in the canonical heat stress response: Hsp90 isoforms Hsp82 and Hsc82, and the Hsp70 family members Ssa1 and Ssa2. Hsc82 and Ssa2 are orthologs of the human HSPs most

commonly found in EVs, based on proteomic studies (Wyciszkiewicz et al., 2019). Interestingly, when I examined abundance of these proteins in EVs collected during heat or hypoosmotic stress, I found that both were enriched in EVs secreted during sublethal heat stress (**Figure 8B**). This finding suggests that high levels of protein chaperones, such as Ssa2 and Hsc82, shared by EVs may protect yeast cells from lethal heat stress.

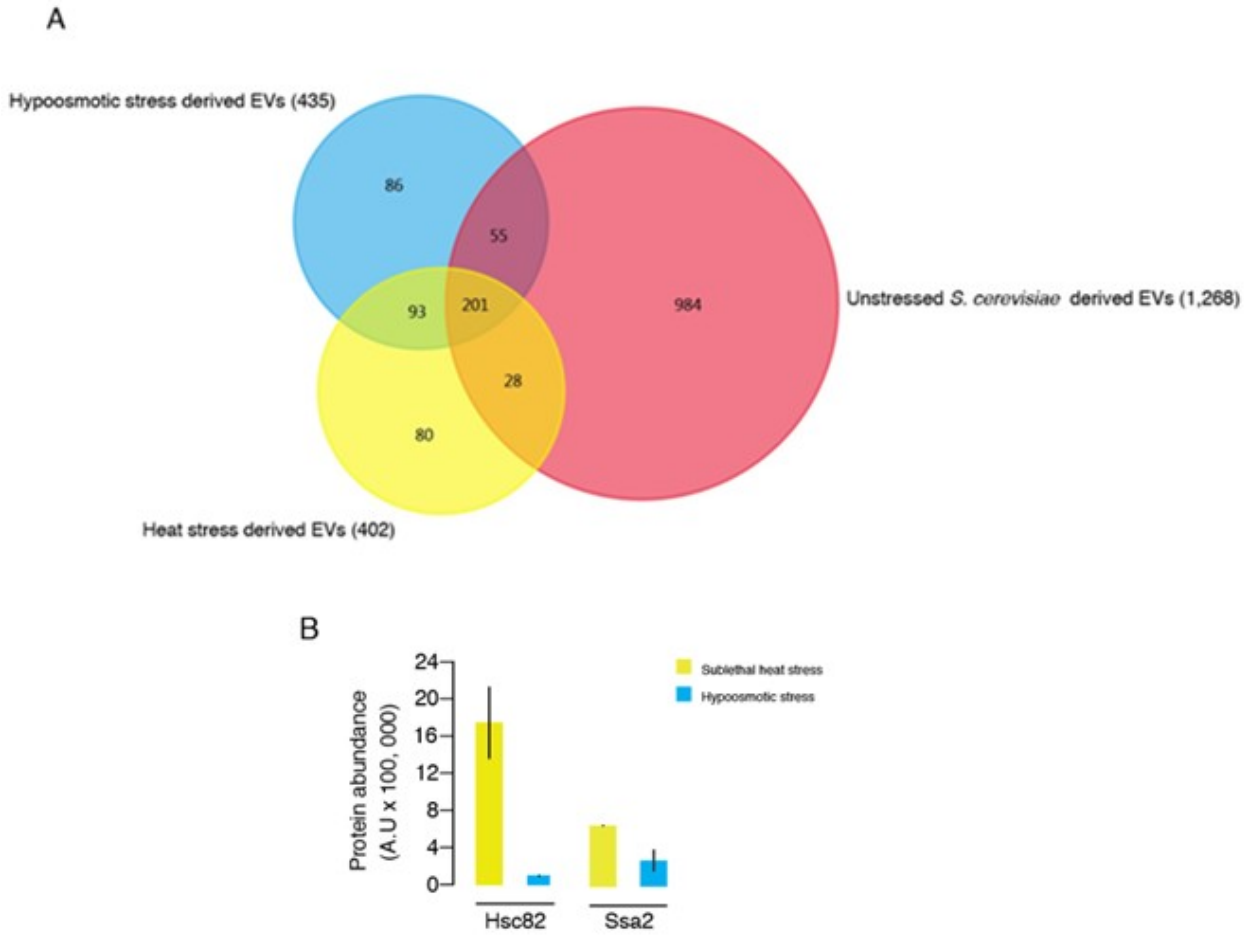

Figure 8. Protein identification of EVs isolated from stress - specific conditions

(A) Venn diagram depicting overlap of proteins detected in EV fractions from stress conditions compared to proteins identified in *S. cerevisiae* based studies documented on Vesiclepedia. **(B)** Protein enrichment analysis of EV fractions collected from heat stress conditions compared to hypoosmotic stress conditions (n=2). Mean ± S.E.M shown.

3.7 Chaperones Hsc82 and Ssa2 are necessary for EV-mediated protection from heat stress

Given that the protein chaperones Hsc82 and Ssa2 play critical roles in clearing toxic misfolded proteins, and that they are abundant in EVs, I hypothesized that they contribute to EV-mediated protection from heat stress (**Figure 2**). To test this hypothesis, I collected EVs from donor cells lacking *HSC82* or *SSA2* and predicted that they would not confer protection against heat stress. After using QELS analysis to confirm that EVs collected from mutants did not differ in mean diameter (**Figure 9A**), I repeated the bioactivity assay and found that EVs from *hsc82*Δ or *ssa2*Δ donor cells showed a diminished protective effect (**Figure 9B**). This result suggests that EVs share protein chaperones between yeast cells to help protect against proteotoxicity by heat stress.

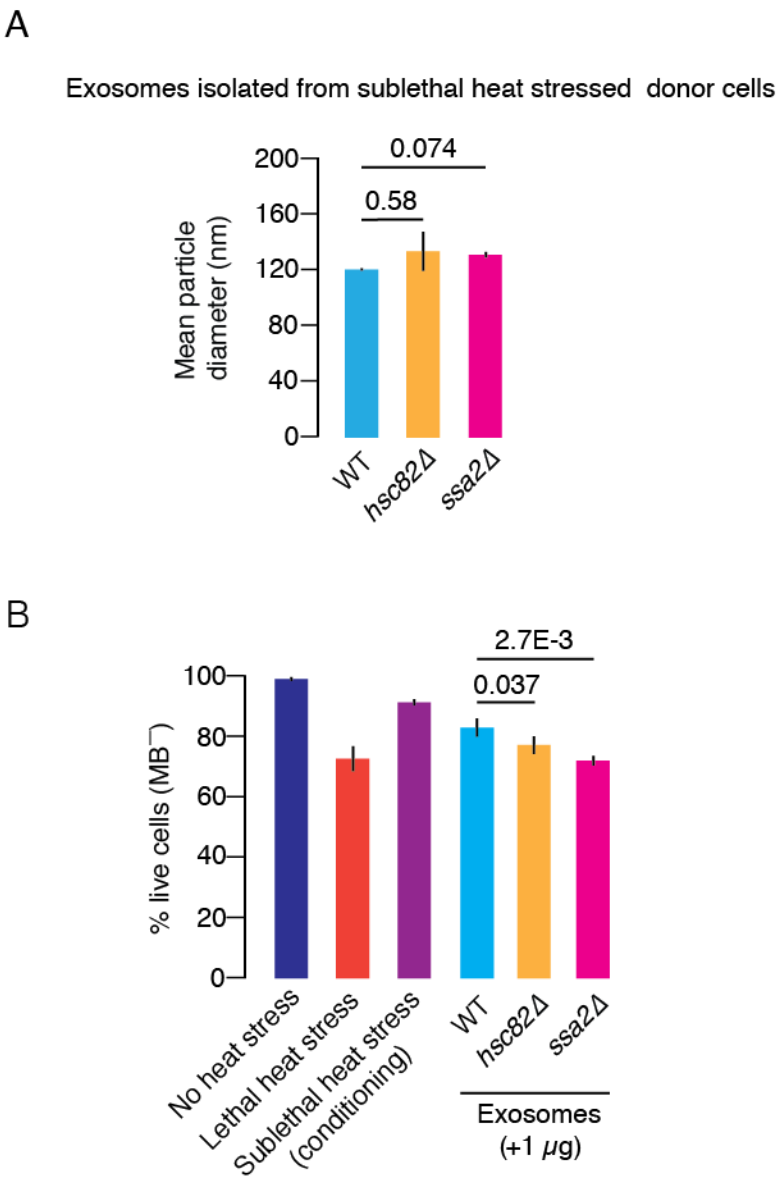

Figure 9. Hsc82 and Ssa2 depleted EVs do not confer protection against heat stress

(A) Results from QELS analysis are shown, to provide preliminary confirmation of isolated EVs from donor cells lacking *HSC82 or SSA2* (n = 3). **(B)** Proportion of methylene blue-negative stained WT recipient cells treated with EVs derived from either WT donor cells or donor cells lacking heat shock proteins hsc82 or ssa2 was determined (n = 3). Mean ± S.E.M. and *P*-values from two-tailed Student t-tests shown are shown.

Chapter 4: Discussion

4.1 Intercellular communication by EVs protects cells from proteotoxicity triggered by heat stress

As previous studies have demonstrated, insoluble protein aggregates are deleterious to cell survival (Wickner, 2016). However, cells have developed protein quality control mechanisms to mitigate the damaging effects of misfolded proteins (Fulda et al., 2012). Of the many biological processes involved, HSPs are critical for eradicating cells of misfolded proteins. However, the ability of cells to prevent proteotoxicity is not limited to the intracellular niche (Hessvik et al., 2018). EV-mediated signaling enables the sharing of prosurvival information between cells and appears to provide protection against environmental challenges, such as salt stress and heat stress (Bewicke-Copley et al., 2017; Zhao et al., 2019). Further dissection of this pathway illustrated that HSPs are shared between cells via EV signalling and elicit a pro-survival response over and above that conferred by the canonical chaperone driven intracellular heat stress response pathway (Morano et al., 2012). Herein, I show that EVs are secreted into the environment from *S. cerevisiae* during mild heat stress, a trigger of proteostasis (**Figure 3**). These EVs are exosomes, as they are membrane-bound particles, ~120 nm diameter in size and contain Bro1, the yeast ortholog of ALIX (**Figure 3 and 4**). These exosomes are then readily taken up (within minutes) by recipient cells though endocytosis (**Figure 5**). Here, they trigger a response that protects cells from lethal heat stress (**Figure 6 and 7**). Moreover, this response appears to be dependent on two enriched exosomal cargo proteins, Hsc82 and Ssa2, which are key protein chaperones known to prevent proteotoxicity (**Figure 8 and 9**). Thus, intercellular communication by exosomes plays a previously underappreciated but important role in protecting the *S. cerevisiae* population from proteotoxicity.

Since the discovery of EVs, scientists realized that not all of them contribute to intercellular communication. Some larger EVs are simply products of cell death for example (Maas et al., 2018). Thus, it is possible that this is also the case for some EVs released during heat stress because: (1) yeast cells would be more likely to survive if they clear toxic proteins that form under heat stress by sequestering them into EVs for release into the environment; or (2) EVs are valuable sources of nutrients, and their endocytosis and catabolism may help rebuild

cells recovering from proteotoxic shock, promoting survival. However, it is unlikely that observed EVs are products of cell death, as yeast culture viability was not affected by sublethal heat stress as compared to unstressed conditions (**Figure 3**), and the mean diameter of the EV population was much smaller than apoptotic bodies (500 – 1,000 nm) (**Figure 4**; Maas et al., 2018; Zhao et al., 2019).

Rather, most evidence presented support the idea that exosomes drive protection from proteotoxicity, including three key findings: (1) isolated exosomes (collected from a different yeast culture under heat stress) added to naïve, unstressed cells are endocytosed and are sufficient to completely protect cells in place of conditioning (**Figure 5 and 6**). Thus, toxic protein shedding by EVs does not exclusively contribute to this response; otherwise these exosomes would not have bioactivity. (2) Adding exosome collected during hypoosmotic stress does not confer protection (**Figure 7**), eliminating the possibility that EVs taken up by cells are simply a nutrient source to support recovery and survival. (3) In support, adding isolated exosomes devoid of chaperones Hsc82 or Ssa2 reduces their protective effect on wild-type, naïve yeast cells (**Figure 9**). This result also begins to reveal mechanistic underpinnings, as these are key enzymes for protein refolding necessary for toxic protein aggregate disassembly.

4.2 Basis of EV communication is dependent on environmental stressor

Prior to this study, researchers only collected EVs from *S. cerevisiae* or pathogenic fungi under unstressed conditions and for 16 – 41 hours during multiple, different stages of culture growth, and found that they have bioactivity (Liu et al., 2016; Rodrigues et al., 2019; Zhao et al., 2019). The same is true for most studies that collect diverse, mixed EVs from patient or animal samples whereby the donor cells are often unknown as well (Bewicke-Copley et al., 2017; Harmati et al., 2019). On the other hand, acute stressors were shown to affect size and composition of EV communities released by cultured mammalian cells, but specific bioactivities of these different EV populations remain unclear (Takahashi et al., 2017). As such, this has led to a debate in the field whether there are universal EVs constitutively released that mediate diverse cellular responses, or there are unique EV populations that are selectively released to mediate

specific physiological events. Based on published work both likely exist, but this study offers strong support for the latter model by offering the following key evidence:

First, I find that EV release from *S. cerevisiae* occurs constitutively, but it is stimulated by sublethal heat stress or hypoosmotic stress (**Figure 7**), suggesting donor yeast cells sense and respond to stressors to release EVs, probably by regulating the MVB-plasma membrane fusion machinery, akin to conventional regulated exocytosis (e.g. synaptic vesicle fusion). Second, EVs released were between 80 – 120 nm in diameter (**Figure 4**), suggesting only exosomes are selectively released, not other larger EVs. Third, exosomes released under the two conditions had different protein compositions (**Figure 8**), suggesting they represent different populations and inferring that protein sorting during biogenesis can be regulated. Forth, exosome release was additive when different stressors were applied in tandem (**Figure 7**), suggesting that donor cells may have multiple pools of EVs and release of each is separately triggered. Fifth, exosome uptake by endocytosis was stimulated by heat stress (**Figure 5**), which is required for efficient intercellular communication by EVs under this condition. Lastly, only exosomes collected under mild heat stress exhibited protection against subsequent lethal heat stress (**Figure 6 and 9**), confirming that stressor-specific release is essential for selective bioactivity. To my knowledge, this study is the first to demonstrate specificity of stress triggered EV communication from release to response in *S. cerevisiae*.

4.3 Unique, enriched and common proteins for EV signaling during heat stress

To further understand the function of EVs, it is important to identify their biomolecular composition (proteins, lipids, nucleic acids). In this study, I compared heat stress derived EVs with existing *S. cerevisiae*-derived EV proteomic studies (Oliveira et al., 2010; Zhao et al., 2019) in which I detected 229 commonly shared proteins (**Figure 8**). Of these 229 proteins, frequently reported EV biomarkers in fungal studies were detected, including glucan 1, 3-β -glucosidases and enolases (**Table S1**). This supports previous hypotheses concerning *trans*-cell wall transport in which EVs containing cell wall modifying enzymes would facilitate local disassembly of the cell wall to improve passage (Brown et al., 2015). Interestingly, enolases have been reported to

be enriched in cancer cell-derived exosomes which enhanced metastasis (Didiasova et al., 2019). Detection of these glycolytic enzymes in *S. cerevisiae*-derived EVs would suggest an existing orthology between selective EV cargo sorting between yeast and human systems in stress inducing conditions. In further support, eukaryotic translation initiation factor (EIF) Sui1 and 40S ribosomal subunit Rps28 were detected in EVs derived from heat-stressed *S. cerevisiae* (**Table S2**). EIFs have been previously reported to be enriched in EVs derived from brain endothelial cells subjected to pro-inflammatory cytokine tumour necrosis factor (TNF) treatment (Dozio and Sanchez, 2017; Yang et al., 2018). It has been also demonstrated that RNA species are detected in EV fractions derived from human embryonic kidney cells (Di Liegro et al., 2017; Sork et al., 2018). Moreover, I detected phosphoglycerate kinase Pgk1 and glyceraldehyde-3-phosphate dehydrogenase Tdh3 which are commonly reported EV biomarkers in pathogenic fungi including: *C. neoformancs, P. brasiliensis,* and *H. capsulatum* although their virulent function is understudied (Vallejo et al., 2012).

Finally, of the 229 shared proteins between heat stress-derived EVs (this study) and unstressed *S. cerevisiae*-derived EVs available on Vesiclepedia (**Figure 8**); indicated peptide coverage and protein abundance suggested that HSPs Hsc82 and Ssa2 are enriched in EVs released during heat stress (**Table S1**). Additionally, HSPs Hch1, Hsp82 and Ssa1 were identified and have been also shown to be bioactive components of human-derived EVs in response to heat stress conditions (**Table S1 and S2**) (De Maio and Vazquez, 2013; Bewicke-Copley et al., 2017; Lauwers et al., 2018; Reddy et al., 2018). Thus, provided such evidence would warrant further study of these proteins in which I speculate are critical to prevent proteotoxicty (**Figure 2**).

4.4 EVs may represent an altruistic mechanism for protecting cell communities from proteotoxicity

Does an individual cell optimize population survival when challenged with stress? As previously demonstrated, EVs harvested from non-stressed *S. cerevisiae* donor cells were shown to rescue stressed cell wall defective recipient cell populations (Zhao et al., 2019). Furthermore,

heat stress-derived EVs from epithelial cells were shown to promote pro-survival responses in naïve cells following repeated cycles of stress (Bewicke-Copley et al., 2017). Together, these findings are in support of the bystander effect phenomenon; which describes naïve cells exhibiting signs of stress when introduced to previous stressed cells. I speculate within this biological phenomenon exists an altruistic mechanism, which in a cell population; acting donor cells release EVs to enhance survival of surrounding cells challenged with stress, however, in the process; donor cells are at the disadvantage to having to bear the sole responsibility of functioning as EV suppliers.

To my knowledge, this hypothesis has not been formally tested. However, this proposition seems reasonable through devising strategies to identify separate EV donor or recipient cell populations. In this study, I confirmed the release of EVs through loss of intracellular GFP fluorescence of EV biomarker Bro1, however, not all cells were depleted of Bro1 puncta and thus, revealing two populations – those that showed loss in fluorescence are donors (**Figure 3**). Moreover, I demonstrated that Bro1-GFP enriched EVs are readily internalized by recipient cells (**Figure 5**) and again I find that some cells uptake EVs more readily relative to other nearby cells that do not – whereby cells that do likely represent recipient cells (**Figure 5**). I speculate that what differentiates donor cells and recipient cells could be dependent on expression levels of HSPs. Perhaps EV donor cells are cells that are aged and have undergone intracellular changes as a result of previous stress exposure, thus exhibiting greater HSP expression. On the contrary, EV recipient cells can be defined as young, naïve cells that minimally express HSPs. A possible strategy to test this hypothesis is to use a single cell sorting approach to cell cultures with and without fluorescently labeled HSPs in order to potentially distinguish EV donor and recipient cell populations. For example, I expect that young cells with low HSP levels should not release EVs and not respond to applied heat stress. In sum, I anticipate that the proposed altruistic mechanism hypothesis is critical for propagating proteostatic information (HSPs) to naïve, younger cells in order to ensure population survival when challenged with lethal stressors.

4.5 Broader physiological relevance

The canonical intracellular heat stress response pathway was first discovered, in part, and characterized in molecular detail in *S. cerevisiae* (Lindquist and Craig, 1988). It is critical for preventing proteotoxicity in all eukaryotic species studied, including humans where it counters aging and pathological processes. As previously reported, any dysfunction in this pathway can induce and exacerbate neurodegenerative diseases such Alzheimer's and prion-based diseases including Creutzfeldt-Jakob disease and Gerstmann-Straussler-Scheinker syndrome (Knight and Will, 2004; Klohn et al., 2013). Herein, I show using *S. cerevisiae* as a model that HSP sequestering exosomes are shared among cells subjected to heat stress and support the notion that EV mediated intercellular communication further contributes to mitigating the deleterious effects of proteotoxic stress.

Consistent with my studies, EVs have been shown to be direct mediators of the bystander effect phenomenon in which EVs isolated from heat stressed breast cancer cell lines reduced DNA damage and apoptosis in surrounding non-stressed cells. On the contrary, heat stress-induced EV secretion also promoted pro-metastatic affects in naïve neighboring cell populations (Bewicke-Copley et al., 2017). Therefore, I speculate an existing orthology between *S. cerevisiae* and human systems on the basis of EV-mediated cell-cell communication in stress-inducing environments and overall contribution to both eukaryotic cell survival and programmed cell death.

EV-mediated cell-cell signaling has been also implicated in the progression of certain neurodegenerative disorders, such as Alzheimer's disease (Lee et al., 2011). In brief, tau propagation is a major catalyst in the progression of Alzheimer's disease in which resident microglia aid in tau spread via direct exosome secretion (Asai et al., 2015). This observation reinforces the notion that EV-based communication can be exploited by pathogenic elements as means to maintain or exacerbate pathogenesis. Notably, the *S. cerevisiae* Sup35 cytosolic prion protein has been shown to be sequestered in EVs and in which subsequently induces the priogenic phenotype in neighboring recipient cells upon internalization (Kabani and Melki, 2015; Liu et al., 2016). Thus, I show that *S. cerevisiae* can serve as an exceptional model to further dissect the molecular machinery underlying accelerated EV-mediated intercellular

communication in cellular homeostasis and progression of neurodegenerative diseases (Cervenakova et al., 2016).

In addition, regarding how pathogenic fungi release EVs which intensifies the degree of fungal colonization and dissemination within host tissues (da Silva et al., 2016). I suspect that pathogenic fungi release EVs in response to environmental cues to either enhance infectivity or protection against fungicidal host immune responses. Therefore, I speculate that non-pathogenic *S. cerevisiae* can also serve as a model to identify the biogenic and cargo sorting mechanisms responsible for the synthesis of virulent EVs and provide a better understanding of opportunistic fungal infections in molecular detail.

4.6 Future directions

In addition to better elucidating the physiological relevance of EVs to eukaryotic physiology, I helped establish *S. cerevisiae* as a platform to further study EVs, which can be used to address several outstanding questions in the immediate future:

What are the molecular mechanisms responsible for biosynthesis of different EV subtypes? Currently, three principle EV categories are proposed based on size, composition and biogenic origin: exosomes, ectosomes and apoptotic bodies (Coelho and Casadevall, 2019). For example, exosomes are thought to be products of MVB maturation, an ESCRT driven process (Wubbolts et al., 2003; Teis et al., 2008; Colombo et al., 2013; Coelho and Casadevall, 2019). But EVs resembling exosomes continue to be released from *S. cerevisiae* mutants devoid of ESCRT genes and show bioactivity (Zhao et al., 2019). These findings suggest that an ESCRT-independent process may also biosynthesize this EV subtype. In this study, I propose that exosomes are responsible for observed bioactivity although I did not implicate ESCRTs or identify the machinery responsible for biogenesis of these exosomes. However, exosome release during osmotic stress did not correlate with Bro1-GFP levels suggesting the involvement of an ESCRT-independent mechanism. In the future, harvesting and studying EVs from yeast cells lacking ESCRT genes will enable us to determine if traditional exosomes mediate the observed response. If not, this will facilitate the discovery of alternative mechanisms responsible for these

exosomes. The discovery of this new machinery would potentially reveal the basis of how different exosome sizes are achieved, or how different cargoes are packaged, and refine our knowledge of this important EV category implicated in many human diseases.

What molecular mechanisms are responsible for EV recognition by recipient cells? EV uptake still occurs within endocytic defective mutants (Delenclos et al., 2017). I speculate that the protein, lipid and sugar laden membrane surface of EVs could reveal potential mechanisms. For example, surface glycans have been reported to be involved in the initial stages of EV-recipient cell interaction using murine hepatic cell lines as models (Williams et al., 2019). Being that EV-mediated cell-cell communication is evolutionary conserved I hypothesize that the enzymatic removal of *N*-glycan groups from heat-stressed derived EVs would inhibit their uptake by naïve cells and subsequent initialization of the pro-survival response. The acquisition of such a result would be the first step forward in engineering the surface membrane of *S. cerevisiae*-derived exosomes and could begin to reveal the types of mechanisms responsible for host cell specific targeting by fungal pathogen EVs or how specific human cell populations communicate using EVs.

Can human EV biogenic pathways functionally replace those of *S. cerevisiae*? It has been well documented that mammalian EVs are required for neuronal communication, tumor metastasis and antigen presentation (Valadi et al., 2007; Harmati et al., 2019). In the case of fungal EVs, studies have demonstrated their ability to effectively carry virulence factors and drive complex immunogenic responses of host tissues with pathological effects (Rodrigues et al., 2008; Brown et al., 2015). Here using yeast, I demonstrated that EV-mediated intercellular communication is an additional stress response to prevent proteotoxicity as reported in human systems, further supporting an existing homology in both mammalian EV and fungal EV lifecycles (Bewicke-Copley et al., 2017). Thus, I speculate that bioactive molecular components (proteins, lipids, sugars and nucleic acids) of yeast exosomes can be functionally replaced by their respective human counterparts. I anticipate this strategy will introduce novel functionalities of newly engineered *S. cerevisiae*-derived exosomes with the potential of serving as therapeutic platforms (Morishita et al., 2017; Li et al., 2018).

References

Alam, S.L., Sun, J., Payne, M., Welch, B.D., Blake, B.K., Davis, D.R., Meyer, H.H., ... and Sundquist, W.I. (2004) Ubiquitin interactions of NZF zinc fingers. *EMBO J*. 23, 1411-1421. doi:10.1038/sj.emboj.7600114

Albuquerque, P.C., Nakayasu, E.S., Rodrigues, M.L., Frases, S., Casadeavll, A., Zancope-Oliveira, R.M., Almeida, I.C., and Nosanchuk, J.D. (2008) Vesicular transport in *Histoplasma capsulatum*: an effective mechanism for trans-cell wall transfer of proteins and lipids in ascomycetes. *Cellular Microbiology*. 10(8), 1-16. doi: 10.1111/j.1462-5822.2008.01160.x

Anderson, J., Mihalik, R., and Soll, D.R. (1990) Ultrastructure and antigenicity of the unique cell wall pimple of the Candida opaque phenotype. *J Bacteriol*. 172(1), 224-235. doi:10.1128/jb.172.1.224-235.1990

Asai, H., Ikezu, S., Tsunoda, S., Medalla, M., Luebke, J., Haydar, T., Wolozin, B., ... and Ikezu, T. (2015) Depletion of microglia and inhibition of exosome synthesis halt tau propagation. *Nature neuroscience*. 18(11), 1584-1593. doi: 10.1038/nn.4132

Babst, M., Katzmann, D.J., Estepa-Sabal, E.J., Meerloo, T., and Emr S.D. (2002) Escrt-III: an endosome-associated heterooligomeric protein complex required for mvb sorting. *Dev Cell*. 3, 271-282. doi: 10.1016/s1534-5807(02)00220-4

Bacon, K., Blain, A., Burroughs, M., McArthur, N., Rao, B.M., and Menegatti, S. (2020) Isolation of Chemically Cyclized Peptide Binders Using Yeast Surface Display. *American Chemical Society Combinatorial Science.* 22(10), 519-532. doi: 10.1021/acscombsci.0c00076

Baietti, M.F., Zhang, Z., Mortier, E., Melchior, A., Degeest, G., Geeraerts, A., Ivarsson, Y., ... David, G. (2012) Syndecan-syntenin-ALIX regulates the biogenesis of exosomes. *Nat Cell Biol*. 14, 677-685. doi:10.1038/ncb2502

Baltazar, L.M., Zamith-Miranda, D., Burnet, M.C., Choi, H., Nimrichter, L., Nakayasu, E.S., and Nosanchuk, J.D. (2018) Concentration-dependent protein loading of extracellular vesicles released by *Histoplasma capsulatum* after antibody treatment and its modulatory action upon macrophages. *Scientific Reports*. 8 (8065), 1-10. doi: 10.1038/s41598-018-25665-5

Bewicke-Copley, F., Mulcahy, L.A., Jacobs, L.A., Samuel, P., Akbar, N., Pink, R.C., and Carter, D.R.F. (2017) Extracellular vesicles released following heat stress induce bystander effect in unstressed populations. Journal of Extracellular Vesicles. 6(1340746), 1-10. doi: 10.1080/20013078.2017.1340746

Bielska, E., Birch, P.R.J., Buck, A.H., Abreu-Goodger, C., Innes, R.W., Jin.H., Pfaffl, M.W., … Weiberg, A. (2018) Highlights of the mini-symposium on extracellular vesicles in inter-organismal communication. *Journal of Extracellular Vesicles*. (8)1 1-8. doi: 10.1080/20013078.2019.1590116

Brett, C.L., Plemel, R.L., Lobinger, B.T., Vignali, M., Fields, S., and Merz, A.J. (2008) Efficient termination of vacuolar Rab GTPase signaling requires coordinated action by a GAP and a protein kinase. *Journal of Cell Biology*. 182(6), 1141-1151. doi: 10.1083/jcb.200801001

Brown, L., Wolf, J.M., Prados-Rosales, R., and Casadevall, A. (2015) Through the wall: extracellular vesicles in Gram-positive bacteria, mycobacteria and fungi. *Nature Reviews Microbiology*. 1-11. doi: 10.1038/nrmicro3480

Buysse, D., Pfitzner, A.K., West, M,.Roux. A., and Odorizzi, G. (2020) The ubiquitin hydrolase Doa4 directly binds Snf7 to inhibit recruitment of ESCRT-III remodeling factors in *S. cerevisiae*. *J Cell Sci*. 133, 1-12. doi:10.1242/jcs.241455

Casadevall, A., Nosanchuk, J.D., Williamson, P., and Rodrigues, M.L. (2009) Vesicular transport across the fungal cell wall. *Trends in Microbiology*. 17, 158-162. doi: 10.1016/j.tim.2008.12.005

Cervenakova, L., Saa, P., Yakovleva, O., Vasilyeva, I., de Castro, J., Brown, P., and Dodd, R. (2016) Are prions transported by plasma exosomes?. *Transfusion and Apheresis Science*. 55, 70–83. doi: 10.1016/j.transci.2016.07.013

Chang, Y.C., & Kwon-Chung, K.J. (1998) Isolation of the third capsule-associated gene, CAP60, required for virulence in Cryptococcus neoformans. *Infect. Immun*. 66, 2230–2236.

Chang, Y.C., and Kwon-Chung, K.J. (1999) Isolation, characterization, and localization of a capsule-associated gene, CAP10, of Cryptococcus neoformans. *J. Bacteriol*. 181, 5636–5643.

Chargaff, E., & West, R. (1946). The Biological Significance of the Thromboplastic protein of blood. *Journal of Biological Chemistry*. 166, 189-197.

Chernoff, Y.O., Newman, G.P., Kumar, J., Allen, K., & Zink, A.D. (1999) Evidence for a protein mutator in yeast: role of the Hsp70-related chaperone ssb in formation, stability, and toxicity of the [PSI] prion. *Molecular and cellular biology*. 19(12), 8103-8112. doi: 10.1128/mcb.19.12.8103

Choi, D.S., Kim, K.D., Kim, Y-.K., and Gho, Y.S. (2014) Proteomics of extracellular vesicles: Exosomes and ectosomes. *Mass Spectrometry Reviews*. 34, 474-490. doi: 10.1002/mas.21420

Coelho, C., & Casadevall, A. (2019) Answers to naysayers regarding microbial extracellular vesicles. *Biochemical Society Transactions*. 47, 1005-1012. doi: 10.1042/BST20180252

Colombo, M., Moita, C., van Niel, G., Kowal, J., Vigneron, J., Benaroch, P., Manel, N., ... Raposo, G. (2013) Analysis of ESCRT functions in exosome biogenesis, composition and secretion highlights the heterogeneity of extracellular vesicles. *J Cell Sci*. 126, 5553-5565. doi:10.1242/jcs.128868

Cordero, R.J.B., Camacho, E., and Casadevall, A. (2020) Melanization in *Cryptococcus neoformans* requires complex regulation. *mBio*. 11, 1-4. doi: 10.1128/mBio.03313-19

De Maio, A., and Vazquez, D. (2013) Extracellular heat shock proteins: A new location, a new function. *Shock*. 40(4), 239-246. doi: 10.1097/SHK.0b013e3182a185ab

Delenclos, M., Trendafilova, T., Mahesh, D., Baine, A.M., Moussaud, S., Yan, I.K., Patel, T., and McLean, P.J. (2017) Investigation of Endocytic Pathways for the Internalization of Exosome-Associated Oligomeric Alpha-Synuclein. *Front Neurosci*. 11(172), 1-10. doi: 10.3389/fnins.2017.00172

Di Liegro, C.M., Schiera, G., and Di Liegro, I. (2017) Extracellular Vesicle-Associated RNA as a Carrier of Epigenetic Information. *Genes*. 8(10), 1-23. doi: 10.3390/genes8100240

Didiasova, M., Schaefer, L., and Wygrecka, M. (2019) When Place Matters: Shuttling of Enolase-1 Across Cellular Compartments. *Frontiers in Cell and Developmental Biology*. 7(61), 1-11. doi: 10.3389/fcell.2019.00061

Dozio, V., and Sanchez, J.C. (2017) Characterisation of extracellular vesicle-subsets derived from brain endothelial cells and analysis of their protein cargo modulation after TNF exposure. *Journal of Extracellular Vesicles*. 6(1), 1-14. doi: 10.1080/20013078.2017.1302705

Feyder, S., De Craene, J., Bar, S., Bertazzi, D.L., and Friant, S. (2015) Membrane Trafficking in the Yeast *Saccharomyces cerevisiae* Model. *International Journal of Molecular Sciences*. 16, 1509-1525. doi: 10.3390/ijms16011509

Freitas, M.S., Bonato, V.L.D., Pessoni, A.M., Rodrigues, M.L., Casadevall, A., and Almeida, F. (2019) Fungal Extracellular Vesicles as Potential Targets for Immune Interventions. *mSphere*. 4(6), 1-9. doi: 10.1128/mSphere.00747-19

Fulda, S., Gorman, A.M., Hori, O., and Samali, A. (2009) Cellular Stress Responses: Cell Survival and Cell Death. *International Journal of Cell Biology*. 2010, 1-23. doi: 10.1155/2010/214074

Gatti, J.L., Métayer, S., Belghazi, M., Dacheux, F., and Dacheux, J.L. (2005) Identification, Proteomic Profiling, and Origin of Ram Epididymal Fluid Exosome-Like Vesicles. *Biology of Reproduction*. 72, 1452-1465. doi: 10.1095/biolreprod.104.036426

Giardina, B.J., Stein, K., and Chiang, H. (2014) The endocytosis gene *END3* is essential for the glucose-induced rapid decline of small vesicles in the extracellular fraction in *Saccharomyces cerevisiae*. *Journal of Extracellular Vesicles*. 3, 1-11. doi: 10.3402/jev.v3.23497

Giri, P.K., and Schorey, J.S. (2008) Exosomes Derived from M. Bovis BCG Infected Macrophages Activate Antigen-Specific CD4+ and CD8+ T Cells *In Vitro* and *In Vivo*. *Plos One*. 3(6), 1-10. doi: 10.1371/journal.pone.0002461

Harmati, M., Gyukity-Sebestyen, E., Dobra, G., Janovak, L., Dekany, I., Saydam, O., Hunyadi-Gulyas, E., … Buzas, K. (2019) Small extracellular vesicles convey the stress-induced adaptive responses of melanoma cells. *Scientific Reports*. 9(15329), 1-20. doi: 10.1038/s41598-019-51778-6

Hessvik, N.P., and Llorente, A. (2018) Current knowledge on exosome biogenesis and release. *Cell Mol Life Sci*. 75, 193-208. doi:10.1007/s00018-017-2595-9

Huang, S.H., Wu, C.H., Chang, Y.C (2012) Cryptococcus neoformans-derived microvesicles enhance the pathogenesis of fungal brain infection. *PLoS One*. 7, 1-12. doi: 10.1371/ journal.pone.0048570

Huh, W.K., Falvo, J.V., Gerke, L.C., Carroll, A.S., Howson, R.W., Weissman J.S., and O'Shea, E.K. (2003) Global analysis of protein localization in budding yeast. *Nature*. 425, 686-691. doi: 10.1038/nature 02026

Hurley, J.H., and Hanson, P.I. (2010) Membrane budding and scission by the ESCRT machinery: it's all in the neck. *Nat Rev Mol Cell Biol*. 11, 556-566. doi:10.1038/nrm2937

Johansson, H.J., Vallhov, H., Holm, T., Gehrmann, U., Andersson A., Johansson, C., Blom, H., Carroni, M., … Scheynius, A. (2018) Extracellular nanovesicles released from the

commensal yeast *Malassezia sympodialis* are enriched in allergens and interact with cells in human skin. *Scientific Reports*. 8(9182), 1-11. doi: 10.1038/s41598-018-27451-9

Johnson, N., West, M., and Odorizzi, G. (2017) Regulation of yeast ESCRT-III membrane scission activity by the Doa4 ubiquitin hydrolase. *Mol Biol Cell*. 28, 661-672. doi:10.1091/mbc.E16-11-0761

Johnston, G. C., Singer, R. A., and McFarlane, S. E. (1977) Growth and cell division during nitrogen starvation of the yeast *Saccharomyces cerevisiae*. *Journal of Bacteriology*. 132(2), 723-730.

Kabani, M., and Melki, R. (2015) More than just trash bins? Potential roles for extracellular vesicles in the vertical and horizontal transmission of yeast prions. *Current Genetics*. 62, 265-270. doi: 10.1007/s00294-015-0534-6

Kapila, N., Sharma, A., Kishore, A., Sodhi, M., Tripathi, P.K., Mohanty, A.K., and Munesh, M (2016) Impact of Heat Stress on Cellular and Transcriptional Adaptation of Mammary Epithelial Cells in Riverine Buffalo (Bubalus Bubalis). *PLoS One*. 11(9), 1-28. doi: 10.1371/journal.pone.0157237

Karim, M.A., Samyn, D.R., Mattie, S., and Brett, C.L. (2018) Distinct features of multivesicular body-lysosome fusion revealed by a new cell-free content-mixing assay. *Traffic*. 19(2), 138-149. doi: 10.1111/tra.12543

Katzmann, D.J., Babstm M., and Emr, S.D. (2001) Ubiquitin-dependent sorting into the multivesicular body pathway requires the function of a conserved endosomal protein sorting complex, ESCRT-I. *Cell*. 106, 145-155. doi:10.1016/s0092-8674(01)00434-2

Klohn, P., Castro-Seoane, R., and Collinge, J. (2013) Exosome release from infected dendritic cells: a clue for a fast spread of prions in the periphery?. *The Journal of infection*. 67(5), 359-368. doi: 10.1016/j.jinf.2013.07.024

Knight, R.S.G and Will, R.G. (2004) Prion Diseases. *Journal of Neurology, Neurosurgery & Psychiatry*. 75, 36-42. doi: 10.1136/jnnp.2004.036137

Konoshenko, M.Y., Lekchnov, E.A., Vlassov, A.V., and Laktionov, P.P. (2018) Isolation of Extracellular Vesicles: General Methodologies and Latest Trends. *Hindawi*. 1-27. doi: 10.1155/2018/8545347

Kostelansky, M.S., Schluter, C., Tam, Y.Y., Lee, S., Ghirlando, R., Beach, B., Conibear, E., and Hurley, J.H. (2007) Molecular architecture and functional model of the complete yeast ESCRT-I heterotetramer. *Cell*. 129, 485-498. doi:10.1016/j.cell.2007.03.016

Kutralam-Muniasamy,G., Flores-Cotera, L.B., and Perez-Guevara,F. (2015) Potential of yeast secretory vesicles in biodelivery systems. *Drug Discovery Today*. 20(6), 659-666. doi: 10.1016/j.drudis.2015.03.014

Lauwers, E., Wang, Y., Gallardo, R., Van der Kant, R., Michiels, E., Swerts, J., Baatsen, P., ... Verstreken, P. (2018) Hsp90 Mediates Membrane Deformation and Exosome Release. *Cell Press*. *71*, 689-702. doi: 10.1016/j.molcel.2018.07.016

Lindquist, S., Craig, E.A. (1988) The Heat-Shock Proteins. *Annual Review of Genetics*. 22, 631-677. doi: 10.1146/annurev.ge.22.120188.003215

Li,S., Lin, Z., Jiang, X., and Yu, X. (2018) Exosomal cargo-loading and synthetic exosome mimics as potential therapeutic tools. *Acta Pharmologica Sinica*. 39, 542-551. doi: 10.1038/aps.2017.178

Liu, S., Hossinger, A., Hofmann, J.P., Denner, P., and Vorberg, I.M. (2016) Horizontal Transmission of Cytosolic Sup35 Prions by Extracellular Vesicles. MBio. 7(4), 1-12. doi 10.1128/mBio.00915-16.

Liu, S., Hossinger, A., Gobbels, S., and Vorberg, I.M. (2017) Prions on the run: How extracellular vesicles serve as delivery vehicles for self-templating protein aggregates. *Prion*. 11, 98–112. doi: 10.1080/19336896.2017.1306162

Lysangela, A.R., da Silva, R.P., Sanchez, D.A., Zamith-Miranda, D., Rodrigues, M.L., Goldenberg, S., Puccia, R., and Nosanchuk, J.D. (2019) Extracellular Vesicle-Mediated

RNA Release in *Histoplasma capsulatum*. *mSphere*. 4(2), 1-17. doi: 10.1128/mSphere.00176-19

Maas, S.L.N., Breakefield, X.O., ans Weaver, A.M. (2018) Extracellular Vesicles: Unique Intercellular Delivery Vehicles. *Trends Cell Bio*. 27(3), 172-188. doi: 10.1016/j.tcb.2016.11.003

McNally, E.K., and Brett, C.L. (2017) ILF and vReD pathways cooperate to control lysosomal transporter protein lifetimes. *eLife*. 1-34. doi: 10.1101/20439

McNally, E.K., and Brett, C.L. (2018) The intralumenal fragment pathway mediates ESCRT-independent surface transporter down-regulation. *Nature communications*, 1-15. doi: 10.1038/s41467-018-07734-5

Mears, R., Craven, R.A., Hanrahan, S., Totty, N., Upton, C., Young, S.L., Patel, P., ... Banks, R.E. (2004) Proteomic analysis of melanoma-derived exosomes by two-dimensional polyacrylamide gel electrophoresis and mass spectrometry. *Proteomics*. 4, 4019-4031. doi: 10.1002/pmic.200400876

Morano, K.A., Grant, C.M., and Moye-Rowley, W.S. (2012) The response to heat shock and oxidative stress in *Saccharomyces cerevisiae*. *Genetics*. 190(4), 1157-1195. doi: 10.1534/genetics.111.128033.

Morishita, M., Takahashi, Y., Nishikawa, M., and Takakura, Y. (2017) Pharmacokinetics of Exosomes-An Important Factor for Elucidating the Biological Roles of Exosomes and for the Development of Exosome-Based Therapeutics. *Journal of Pharmaceutical Sciences*. 106, 2265-2269. doi: 10.1016/j.xphs.2017.02.030

Monari, C., Pericolini, E., Bistoni, G., Casadevall, A., Kozel, T.R., and Vecchiarelli, A. (2005) *Cryptococcus neoformans* Capsular Glucuroxylommanan Induces Expression of Fas Ligand in Macrophages. *The Journal of Immunology*. 174(6) 3461-3468. doi: 10.4049/jimmunol.174.6.3461

Nimrichter, L., and Rodrigues, M.L. (2011) Fungal glucosylceramides: from structural components to biologically active targets of new antimicrobials. *Front Microbiol*. 2(212), 1-7. doi: 10. 3389/fmicb.2011.00212

Nimrichter, L., de Souza, M.M., Del Poeta, M., Nosanchuk, J.D., Joffe, L., Tavares, P.M., and Rodrigues, M.L. (2016) Extracellular Vesicle-Associated Transitory Cell Wall Components and Their Impact on the Interaction of Fungi with Host Cells. *Frontiers in Microbiology*. 7 (1034), 1-11. doi: 10.3389/fmicb.2016.01034

Oliveira, D.L., Nakayasu, E.S., Joffe, L.S., Guimaraes, A.J., Sobreira, T.J.P, Nosanchuk, J.D, Cordero, R.J.B., … Rodrigues, M.L. (2010) Characterization of Yeast Extracellular Vesicles: Evidence for the Participation of Different Pathways of Cellular Traffic in Vesicle Biogenesis. *Plos One*. 5(6), 1-13. doi: 10.1371/journal.pone.0011113

Oliveira, D.L., Nakayasu, E.S., Joffe, L.S., Guimaraes, A.J., Sobreira, T.J.P, Nosanchuk, J.D, Cordero, R.J.B., … Rodrigues, M.L. (2010) Biogenesis of extracellular vesicles in yeast: many questions with few answers. *Communicative & Integrative Biology*. 3(6), 533-535. doi: 01371/journal.pone.0011113

Oliveira, D.B.L., Nimrichter, L., Miranda, K., Frases, S., Faull, K.F., Casadevall, A., and Rodrigues, M.L. (2009) Cryptococcus neoformans cryoultramicrotomy and vesicle fractionation reveals an intimate association between membrane lipids and glucuronoxylomannan. *Fungal Genet. Biol*. 46, 956–963. doi: 10.1016/j.fgb.2009.09.001

Oliveira, D.L., Friere-de-Lima, C.G., Nosanchuk, J.D., Csadevall, A., Rodrigues, M.L., and Nimrichter, L. (2010) Extracellular Vesicles from *Cryptococcus neoformans* Modulate Macrophage Functions. *Infection and Immunity*. 1601-1609. doi: 10.1128/IAI.01171-09

Oliveira, D.L., Rizzo, J., Joffe, L.S., Godinho, R.M., and Rodrigues. M.L. (2013) Where do they come from and where do they go: candidates for regulating extracellular vesicle formation in fungi. *Int J Mol Sci*. 14, 9581-9603. doi:10.3390/ijms14059581

Pan, B., and Johnstone, R.M. (1983) Fate of the Transferrin Receptor during Maturation of Sheep Reticulocytes In Vitro: Selective Externalization of the Receptor. *Cell*. 33, 967-977. doi: 1016/0092-8674(83)90040-510

Panepinto, J., Komperda, K., Frases, S., Park, Y., Djordjevic, J.T., Casadevall, A., and Williamson, P.R. (2009) Sec6-dependent sorting of fungal extracellular exosomes and laccase of Cryptococcus neoformans. *Mol Microbiol*. 71, 1165-1176. doi: 10.1111/j.1365-2958.2008.06588.x

de Souza Pereira, R., and Geibel, J. (1999) Direct observation of oxidative stress on the cell wall of Saccharomyces cerevisiae strains with atomic force microscopy. *Molecular and cellular biochemistry*. 201 (2), 17-24. doi: 10.1023/a:1007007704657

Perfect, J.R., and Bicanic, T. (2014) Cryptococcosis Diagnosis and Treatment: What Do We Know Now. *Fungal Genetic Bio*. 78, 49-54. doi: 10.1016/j.fgb.2014.10.003

Pillet, F., Lemonier, S., Schiavone, M., Formosa. C., Martin-Yken, H., Francois, J.M., and Dague, E. (2014) Uncovering by Atomic Force Microscopy of an original circular structure at the yeast cell surface in response to heat shock. *BMC Biology*. 12(6), 1-11. doi: 10.1186/1741-7007-12-6

Reddy, V.S., Madala, S.K., Trinath, S., and Reddy, G.B. (2018) Extracellular small heat shock proteins: exosomal biogenesis and function. *Cell Stress and Chaperones*. 23, 441-454. doi: 10.1007/s12192-017-0856-z

Reis, F.C.G., Borges, B.S., Jozefowicz, L.J., Sena, B.A.G., Garcia, A.W.A., Medeiros, L.C., Martins, S.T., ...Rodrigues, M.L. (2019) A Novel Protocol for the Isolation of Fungal Extracellular Vesicles Reveals the Participation of a Putative Scramblase in Polysaccharide Export and Capsule Construction in *Cryptococcus gattii*. *mSphere*. 4(2), 1-15. doi: 10.1128/mSphere.00080-19

Retini, C., Kozel, T. R., Pietrella, D., Monari, C., Bistoni, F., and Vecchiarelli, A. (2001) Interdependency of Interleukin-10 and Interleukin-12 in Regulation of T-Cell

Differentiation and Effector Function of Monocytes in Response to Stimulation with Cryptococcus neoformans. *Infection and Immunity, 69(10), 6064–6073*. doi:10.1128/iai.69.10.6064-6073.2001

Rice, G.E., Scholz-Romero, K., Sweeney, E., Peiris, H., Kobayashi, M., Duncombe, G., Mitchell, M.D., and Salomon, C. (2015) The Effect of Glucose on the Release and Bioactivity of Exosomes From First Trimester Trophoblast Cells. *The Journal of clinical endocrinology and metabolism*. 100(10), 1280-1288. doi: 10.1210/jc.2015-2270

Rider, M.A., Hurwitz, S.N., and Meckes, D.G. (2016) ExtraPEG: A Polyethylene Glycol-Based Method for Enrichment of Extracellular Vesicles. *Scientific Reports*. 6, 1-14. doi: 10.1038/srep23978 (2016)

Rittershaus, P. C., Kechichian, T. B., Allegood, J. C., Merrill, A. H., Jr, Hennig, M., Luberto, C., and Del Poeta, M. (2006) Glucosylceramide synthase is an essential regulator of pathogenicity of Cryptococcus neoformans. *The Journal of clinical investigation*, 116(6), 1651–1659. doi: 10.1172/JCI27890

Rodrigues, M.L., Nimrichter, L., Oliveira, D.L., Nosanchuk, J.D., and Casadevall, A. (2008) Vesicular Trans-Cell Wall Transport in Fungi: A Mechanism for the Delivery of Virulence- Associated Macromolecules? *Lipid Insights*. 2, 27-40. doi: 10.4137/lpi.s1000

Rodrigues, M.L., Nakayasu, E.S., Oliveira, D.L., Nimrichter, L., Nosanchuk, J.D., Almeida, I.C., and Casadevall, A. (2007) Extracellular Vesicles Produced by *Cryptococcus neoformans* Contain Protein Components Associated with Virulence. *Eukaryotic Cell*. 7(1), 58-67. doi: 10.1128/EC.00370-07

Saa, P., Yakovleva, O., de Castro, J., Vasilyeva, I., De Paoli, S.H., Simak, J., and Cervenakova, L. (2014) First Demonstration of Transmissible Spongiform Encephalopathy-associated Prion Protein (PrP^{TSE}) in Extracellular Vesicles from Plasma of Mice Infected with Mouse-adapted Variant Creutzfeldt-Jakob Disease by *in Vitro* Amplification. *The Journal of Biological Chemistry*. 289(42), 29247- 29260. doi: 10.1074/jbc.M114.589564

Sharma, S., LeClaire, M., and Gimzewski, J.K. (2018) Ascent of atomic force microscopy as a nanoanalytical tool for exosomes and other extracellular vesicles. *Nanotechnology*. 29(13), 1-14. doi: 10.1088/1361-6528/aaab06

da Silva, T.A., Roque-Barreira, M.C., Casadevall, A., and Almeida, F. (2016) Extracellular vesicles from *Paracoccidioides brasiliensis* induced M1 polarization. *Scientific Reports*. 6(35867), 1-10. doi: 10.1038/srep35867

Skliar, M., and Chernyshev, V.S. (2019) Imaging of Extracellular Vesicles by Atomic Force Microscopy. *Journal of Visualized Experiments*. 151, 1-13. doi: 10.379159254

Sork, H., Corso, G., Krjutskov, K., Johansson, H.J., Nordin, J.Z., Wiklander, O.P.B., Lee, Y.X.F., ... Andaloussi, S.E. (2018) Heterogeneity and interplay of the extracellular vesicle small RNA transcriptome and proteome. *Scientific Reports*. 8(10813), 1-12. doi: 10.1038/s41598-018-28485-9

Subra, C., Laulagnier, K., Perret, B., and Record, M. (2007) Exosome lipidomics unravel lipid sorting at the level of multivesicular bodies. *Biochimie*. 89, 205-212. doi: 10.1016/j.biochi.2006.10.014

Takahashi, A., Okada, R., Nagao, K., Kawamata, Y., Hanyu, A., Yoshimoto, S., Takasugi, M., … Hara, E. (2017) Exosomes maintain cellular homeostasis by excreting harmful DNA from cells. *Nature Communications*. 8(15287), 1-14. doi: 10.1038/ncomms15287

Takeo, K., Uesaka, I., Nishiura, M. (1974) The Wall Particle of the Genus Cryptococcus: Large Size and Characteristic Distribution. *Journal of General Microbiology*. 84, 223-225. doi: 10.1099/00221287-84-1-223

Teis, D., Saksena, S., and Emr, S.D. (2008) Ordered assembly of the ESCRT-III complex on endosomes is required to sequester cargo during MVB formation. *Dev Cell*. 15, 578-589. doi:10.1016/j.devcel.2008.08.013

Théry, C., Witwer, K.W., Aikawa, E., Alcaraz, M.J., Anderson, J.D., Andriantsitohaina, R., Antoniou, A., ... Zuba-Surma, E.K. (2018) Minimal information for studies of

extracellular vesicles 2018 (MISEV2018): a position statement of the International Society for Extracellular Vesicles and update of the MISEV2014 guidelines. *Journal of Extracellular Vesicles*. 7(1), 1-43. doi: 10.1080/20013078.2018.1535750

Torralba, D., Baixauli, F., and Villarroya-Beltri. (2018) Priming of dendritic cells by DNA-containing extracellular vesicles from activated T cells through antigen-driven contacts. *Nat Commun* 9, 1-17. doi: 10.1038/s41467-018-05077-9

Toribio V., Morales, S., Lopez-Martin, S., Cardenas, B., Cabanas, C., and Yanez-Mo, M. (2019) Development of a quantitative method to measure EV uptake. *Scientific Reports*. 9, 1-14. doi: 10.1038/s41598-019-47023-9

de Toledo Martins, S., Szwarc, P., Goldenberg, S., and Alves, L.R. (2019) Extracellular Vesicles in Fungi: Composition and Functions. *Current Topics in Microbiology Immunology*. 422, 45-59. doi: 10.1007/82_2018_141

Valadi,H., Ekstrom, K., Bossios, A., Sjostrand, M., Lee, J.J., and Lotvall, J.O. (2007) Exosome-mediated transfer of mRNAs and microRNAs is a novel mechanism of genetic exchange between cells. *Nature Cell Biology*. 9(6), 654-659. doi: 10.1038/ncb1596

Vallejo, M. C., Nakayasu, E. S., Matsuo, A. L., Sobreira, T. J. P., Longo, L. V. G., Ganiko, L., … Puccia, R. (2012) Vesicle and Vesicle-Free Extracellular Proteome of Paracoccidioides brasiliensis: Comparative Analysis with Other Pathogenic Fungi. *Journal of Proteome Research*. 11(3), 1676–1685. doi:10.1021/pr200872s

Vargas, G., Rocha, J.D.B., Oliveira, D.L., Albuquerque, P.C., Frases, S., Santos, S.S., and Nosanchuk, J.D. (2015) Compositional and immunobiological analyses of extracellular vesicles released by *Candida albicans*. *Cellular Microbiology*. 17(3), 389–407. doi: 10.1111/cmi.12374

Verghese, J., Abrams, J., Wang, Y., and Morano, K.A. (2012) Biology of the Heat Shock Response and Protein Chaperones: Budding Yeast (*Saccharomyces cerevisiae*) as a

Model System. *Microbiology and Molecular Biology Reviews*. 76(2), 115-158. doi: 10.1128/MMBR.05018-11

Wang, S., Kojima, K., Mobley, J.A., and West, A.B. (2019) Proteomic analysis of urinary extracellular vesicles reveal biomarkers for neurologic disease. *E Bio Medicine*. 45, 351-361. doi: 10.1016/j.ebiom.2019.06.021

Wemmer, M., Azmi, I., West, M., Davies, B., Katzmann, D., and Odorizzi, G. (2011) Bro1 binding to Snf7 regulates ESCRT-III membrane scission activity in yeast. *J Cell Biol*.192, 295-306. doi: 10.1083/jcb.201007018

Wickner, R.B. (2016) Yeast and Fungal Prions. *Cold Spring Harbor Laboratory Press*. 8, 1-15. doi: 10.1101/cshperspect.a023531

Williams, C., Pazos, R., Royo, F., Gonzalez, E., Roura-Ferrer, M., Martinez, A., Gamiz, J., ... Falcon-Perez, J.M. (2019) Assessing the role of surface glycans of extracellular vesicles on cellular uptake. *Scientific Reports*. 9, 1-14. doi: 10.1038/s41598-019-48499-1

Wolf, P. (1967) The Nature and Significance of Platelet Products in Human Plasma. *British Journal of Haemotology*. 13(3), 269-288. doi: 10.1111/j.1365-2141.1967.tb08741.x

Wollert, T., and Hurley, J.H. (2010) Molecular mechanism of multivesicular body biogenesis by ESCRT complexes. *Nature*. 464, 864-869. doi:10.1038/nature08849

Wollert, T., Wunder, C., Lippincott-Schwartz, J., Hurley, J.H. (2009) Membrane scission by the ESCRT-III complex. *Nature*. 458, 172-177. doi:10.1038/nature07836

Wubbolts, R., Leckie, R.S., Veenhuizen, P.T.M., Schwarzmann, G., Mobius, W., Hoernschemeyer, J., Slot, J., ... Stoorvogel,W. (2003) Proteomic and biochemical analyses of human B cell-derived exosomes. Potential implications for their function and multivesicular body formation. *J Biol Chem*. 278(13), 10963-10972. doi:10.1074/jbc.M207550200

Wu, K., Xing, F., Wu, S.Y., and Watabe, K. (2017) Extracellular vesicles as emerging targets in cancer: recent development from bench to bedside. *Biochim Biophys Acta*. 1868(2), 538-563. doi: 10.1016éj.bbcan.2017.10.001

Wyciszkiewicz, A., Kalinowska-Łyszczarz, A., Nowakowski, B., Kaźmierczak, K., Osztynowicz, K., and Sławomir Michalak. (2019) Expression of small heat shock proteins in exosomes from patients with gynecologic cancers. *Scientific Reports*. 9(9817). doi : 10.1038/s41598-019-46221-9

Yang, Y., Boza-Serrano, A., Dunning, C.J.R., Clausen, B.H., Lambertsen, K.L., and Deierborg, T. (2018) Inflammation leads to distinct populations of extracellular vesicles from microglia. *Journal of Neuroinflammation*. 15, 1-19. doi: 10.1186/s12974-018-1204-7

Yang, C., Guo, W.B., Zhang, W.S., Bian, J., Yang, J.K., Zhou, Q.Z., Chen, M.K., ... C.D, Liu. (2017) Comprehensive proteomics analysis of exosomes derived from human seminal plasma. *Andrology*. 5, 1007-1015. doi:10.1111/andr.12412

Yoneda, A., and Doering, T.L. (2006) A eukaryotic capsular polysaccharide is synthesized intracellularly and secreted via exocytosis. *Mol. Biol. Cell*. 17, 5131–5140. doi: 10.1091/mbc.E06-08-0701

Zarnowski, R., Sanchez, H., Covelli, A.S., Dominguez, E., Jaromin, A., Bernhardt, J., Mitchell, K.F., … Andes, D.R. (2018) Candida albicans biofilm-induced vesicles confer drug resistance through matrix biogenesis. *PLoS Biol*. 16(10), 1-18. doi:10.1371/journal.pbio.2006872

Zhang, Y., Jin, X., Liang, J., Guo, Y., Sun, G., Zeng, X., and Yin, H. (2019) Extracellular vesicles derived from ODN-stimulatedmacrophages transfer and activate Cdc42 in recipient cells and thereby increase cellular permissiveness to EV uptake. *Cell Biology*. 5, 1-10. doi: 10.1126/sciadv.aav1564

Zhao, K., Bleackley,M., Chisanga, D., Gangoda, L., Fonseka, P., Liem, M., Kalra, H., … Mathivanan, S. (2019) Extracellular vesicles secreted by *Saccharomyces cerevisiae* are

involved in cell wall remodelling. *Communications Biology*. 2(305), 1-13. doi: 10.1038/s42003-019-0538-8

Supplemental Figures

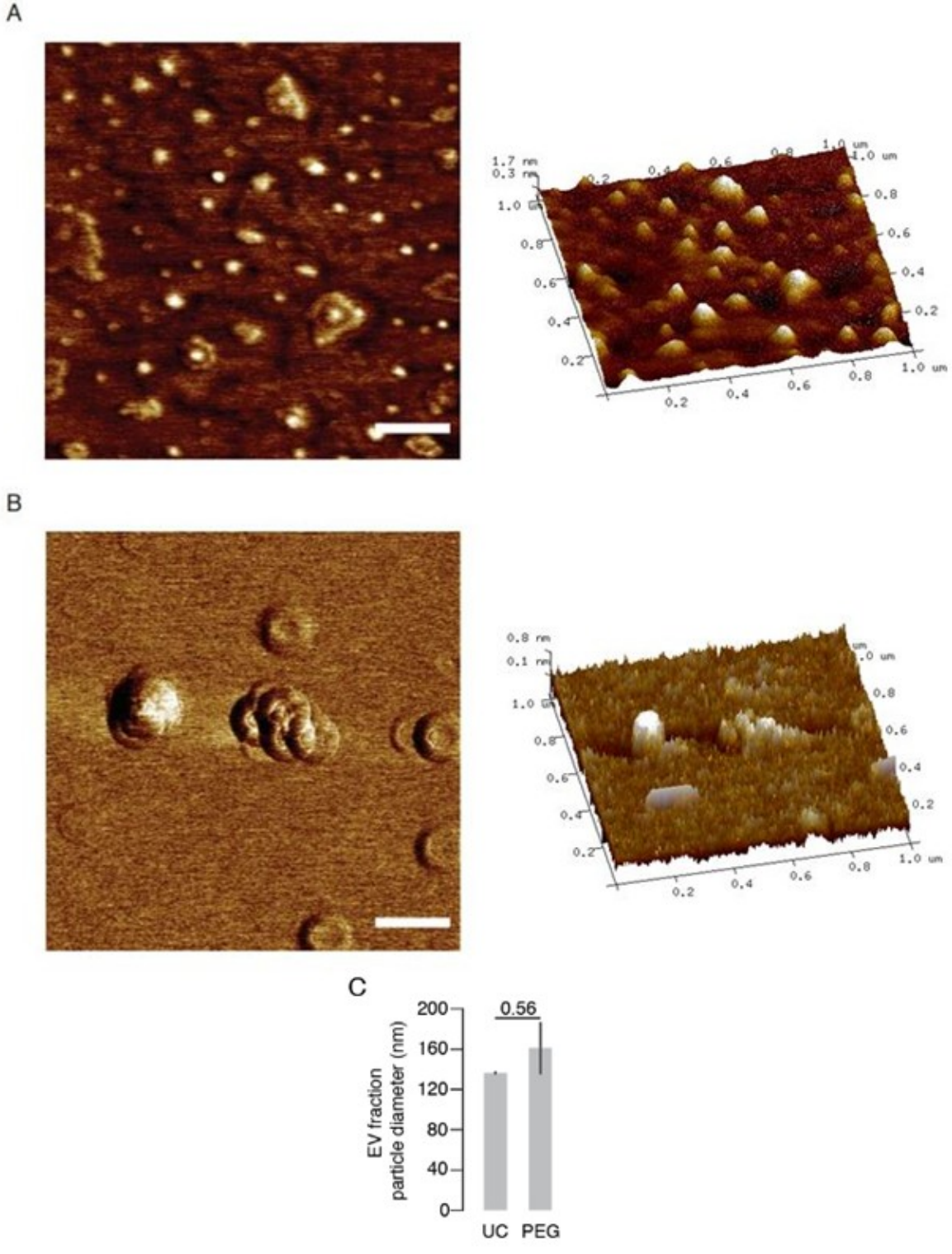

Figure S1. Dimensional analysis of EVs isolated from PEG-based precipitation

(A, B) Phase (left) and topographical mapping (right) images of EV fractions isolated by PEG-based precipitation from yeast cultures during sublethal heat stress in the absence (A) or presence (B) of Triton X-100 acquired using AFM. Examples of 3 independent experiments are shown. **(C)** QELS analysis of EV fractions collected from yeast cells expressing Bro1-GFP either from ultracentrifugation (UC) or PEG-based precipitation (n = 3). Mean ± S.E.M and *P*-value from Student's t-test are shown. Scale bars, 200 nm, 1 µm × 1 µm scan.

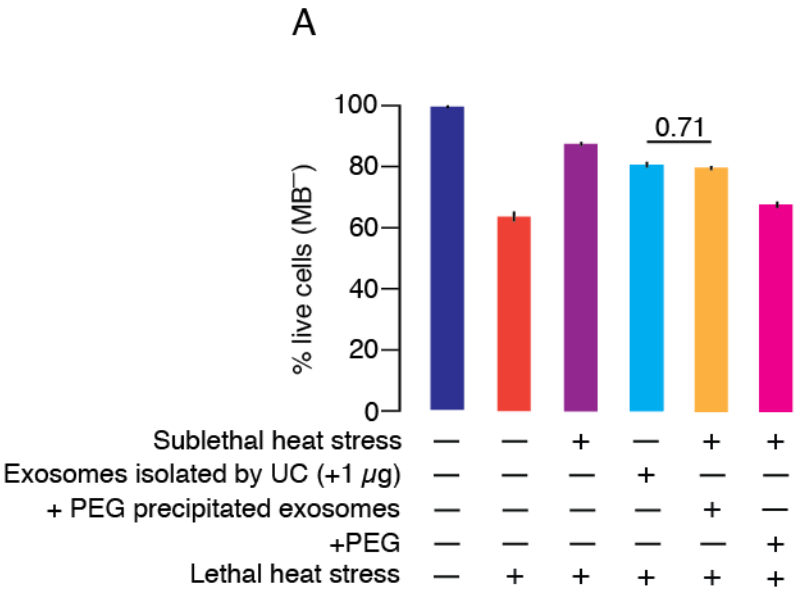

Figure S2. EVs isolated from PEG-based precipitation still protects *S. cerevisiae* cells from lethal heat stress

(A) Proportion of methylene blue-negative cells (live) treated with EVs collected from WT donor cells subjected to sublethal heat stress and isolated by ultracentrifugation (UC) or PEG-based precipitation (n=3). Mean ± S.E.M. and *P*-values from two-tailed Student t-tests shown are shown.

Supplemental Tables

Table S1. Thirty most abundant proteins observed in yeast EV samples

Gene name	Description	# Unique peptides	Abundance
EXG1	glucan 1,3-beta-glucosidase I/II	25	2.63×10^{8}
PGK1	Phosphoglycerate kinase	40	1.36×10^{8}
SCW4	probable family 17 glucosidase SCW4	17	8.46×10^{7}
ENO2	Enolase 2	16	7.86×10^{7}
BGL2	glucan 1,3-beta-glucosidase	12	6.30×10^{7}
ADH1	Alcohol dehydrogenase 1	21	6.07×10^{7}
AHP1	Peroxiredoxin AHP1	14	5.36×10^{7}
PDC1	pyruvate decarboxylase isozyme 1	21	5.24×10^{7}
CPR1	peptidyl-prolyl cis-trans isomerase	10	4.84×10^{7}
PDI1	Protein disulfide-isomerase	22	3.36×10^{7}
FBA1	fructose-bisphosphate aldolase	14	3.20×10^{7}
TPI1	Triosephosphate isomerase	16	3.03×10^{7}
CDC19	Pyruvate kinase 1	27	2.45×10^{7}
GPM1	Phosphoglycerate mutase 1	13	2.24×10^{7}
RHR2	Glycerol-1-phosphate phosphohydrolase 1	12	2.20×10^{7}
ADK1	adenylate kinase	17	2.05×10^{7}
TDH3	Glyceraldehyde-3-phosphate dehydrogenase 3	9	1.51×10^{7}
PHO12	Acid phosphatase PHO12	11	1.39×10^{7}
ADO1	Adenosine kinase	12	1.37×10^{7}
PGI1	glucose-6-phosphate isomerase	19	1.11×10^{7}
GAS3	Probable 1,3-beta-glucanosyltransferase GAS3	10	9.33×10^{6}
TEF1	elongation factor 1-alpha	11	7.80×10^{6}
THR4	threonine synthase	18	6.66×10^{6}
ENO1	Enolase 1	6	5.73×10^{6}
KAR2	78 kDa glucose-regulated protein homolog	18	4.5×10^{6}
HSC82	**ATP-dependent molecular chaperone HSC82**	**6**	$\mathbf{2.32\times10^{6}}$
SSA2	**Heat shock protein SSA2**	**3**	$\mathbf{6.30\times10^{5}}$
TDH2	Glyceraldehyde-3-phosphate dehydrogenase 3	16	4.78×10^{5}

Gene name	Description	# Unique peptides	Abundance
SSA1	**heat shock protein SSA1**	**3**	**3.81×10^5**
HSP82	**ATP-dependent molecular chaperone HSP82**	**2**	**1.89×10^5**

Table S2. Unique proteins in yeast EVs collected during heat stress

Gene name	Description	# Unique peptides	Abundance
ADE8	Phosphoribosylglycinamide formyltransferase	5	1.99×10^7
LTE1	Guanine nucleotide exchange factor	1	1.25×10^7
INP52	Polyphosphatidylinositol phosphatase	1	1.23×10^7
DOG1	2-deoxyglucose-6-phosphate phosphatase 1	3	3.89×10^6
SIR4	Regulatory protein SIR4	1	2.98×10^6
CWP1	Cell wall protein CWP1	6	2.55×10^6
BIK1	Nuclear fusion protein BIK1	1	1.51×10^6
YNL010W	Uncharacterized phosphatase	5	1.31×10^6
UTP9	U3 small nucleolar RNA-associated protein 9	1	9.76×10^5
RSM19	37S ribosomal protein S19, mitochondrial	1	8.23×10^5
HCH1	**Hsp90 co-chaperone**	**2**	**7.32×10^5**
ACB1	acyl-CoA-binding protein	3	6.56×10^5
UBC4	ubiquitin-conjugating enzyme E2 4	1	5.86×10^5
ARL1	ADP-ribosylation factor-like protein 1	4	5.37×10^5
UBC13	Ubiquitin-conjugating enzyme E2 13	3	5.01×10^5
SAR1	Small COPII coat GTPase	1	4.62×10^5
PPX1	Exopolyphosphatase	1	4.44×10^5
YJR098C	Uncharacterized protein	1	4.28×10^5
RPS28A	40S ribosomal protein S28-A	1	3.99×10^5
CYC8	General transcriptional corepressor CYC8	1	3.90×10^5
SUN4	Probable secreted beta-glucosidase	1	3.27×10^5
GRX2	Glutaredoxin-2, mitochondrial	1	3.24×10^5
AIM7	Protein AIM7	1	3.14×10^5
UPF3	nonsense-mediated mRNA decay protein 3	1	2.98×10^5
UTR4	Enolase-phosphatase E1	2	2.85×10^5
RPL6B	60s ribosomal protein l6-b	2	2.08×10^5
MNS1	endoplasmic reticulum mannosyl-oligosaccharide 1,2-alpha-mannosidase	1	2.07×10^5
HUB1	Ubiquitin-like modifier	1	1.72×10^5

Gene name	Description	# Unique peptides	Abundance
GDE1	Glycerophosphocholine phosphodiesterase	1	1.68×10^{5}
AAH1	Adenine deaminase	2	1.67×10^{5}
YDL073W	Upf0592 protein ydl073w	1	1.52×10^{5}
AHK1	Upf0592 protein ydl073w	1	1.52×10^{5}
SOV1	Protein SOV1, mitochondrial	1	1.32×10^{5}
BNA1	3-hydroxyanthranilate 3,4-dioxygenase	1	1.22×10^{5}
HTA2	Histone H2A.2	1	1.17×10^{5}
RTS3	Protein phosphatase type 2A regulatory subunit	1	1.11×10^{5}
YKL033W-A	Putative uncharacterized hydrolase	1	1.10×10^{5}
GPX2	Glutathione peroxidase-like peroxiredoxin 2	1	1.10×10^{5}
YHR131C	PH domain-containing protein	1	1.09×10^{5}
YPT31	GTP-binding protein	1	9.87×10^{4}
AIM29	altered inheritance rate of mitochondria protein 29	2	9.30×10^{4}
LRE1	Laminarase-resistance protein	1	9.04×10^{4}
YKR015C	Uncharacterized protein YKR015C	1	7.89×10^{4}
SUI1	eukaryotic translation initiation factor eIF-1	1	7.72×10^{4}
STM1	Suppressor protein STM1	1	7.61×10^{4}
PAN3	PAN2-PAN3 deadenylation complex subunit PAN3	1	7.05×10^{4}
MNT4	Probable alpha-1,3-mannosyltransferase MNT4	1	6.51×10^{4}
SEE1	Protein-lysine N-methyltransferase efm4	1	6.46×10^{4}
EFM4	Protein-lysine N-methyltransferase efm5	1	6.46×10^{4}
NAS6	probable 26S proteasome regulatory subunit p28	1	6.45×10^{4}
PBI2	Protease B inhibitor 2	1	5.31×10^{4}
YRB1	Ran-specific GTPase-activating protein 1	1	5.21×10^{4}
GUA1	GMP synthase [glutamine-hydrolyzing]	1	5.09×10^{4}
ARC1	tRNA-aminoacylation cofactor ARC1	1	4.82×10^{4}
VMR1	ABC transporter ATP-binding protein/permease	1	4.75×10^{4}
RPS25A	40S ribosomal protein S25-A	1	4.30×10^{4}
HIS6	1-(5-phosphoribosyl)-5-[(5-phosphoribosylamino)methylideneamino] imidazole-4-carboxamide isomerase	1	4.12×10^{4}
YLR126C	Putative glutamine amidotransferase	1	4.04×10^{4}
SRP72	Signal recognition particle subunit SRP72	1	3.51×10^{4}
ECM30	Protein ECM30	1	2.99×10^{4}
RPS29A	40S ribosomal protein S29-A	1	2.69×10^{4}
YLR118C	Acyl-protein thioesterase 1	1	1.56×10^{4}
HSM3	DNA mismatch repair protein HSM3	1	8.40×10^{4}
FCY1	Cytosine deaminase	1	6.47×10^{4}
FUS1	Nuclear fusion protein FUS1	1	6.25×10^{4}

Gene name	Description	# Unique peptides	Abundance
YCR051W	Ankyrin repeat-containing protein	1	-
PLB2	lysophospholipase 2	1	-
NHP6B	Non-histone chromosomal protein 6B	1	-
SRP1	Importin subunit alpha	1	-
YLR225C	Uncharacterized SVF1-like protein	1	-
ZWF1	Glucose-6-phosphate 1-dehydrogenase	1	-
DED1	ATP-dependent RNA helicase		-
SPO74	Sporulation-specific protein 74	1	-
MGA2	protein MGA2	1	-
CET1	mRNA-capping enzyme subunit beta	1	-
GRX5	Monothiol glutaredoxin-5, mitochondrial	1	-
ARO9	Aromatic amino acid aminotransferase 2	1	-
CDC33	Eukaryotic translation initiation factor 4E	1	-
HDA1	Histone deacetylase HDA1	1	-
RRM3	ATP-dependent DNA helicase RRM3	1	-